

PLRV-O: Advancing Differentially Private Deep Learning via Privacy Loss Random Variable Optimization

Qin Yang*
University of Connecticut
Storrs, USA

Nicholas Stout*
Iowa State University
Ames, USA

Meisam Mohammady
Iowa State University
Ames, USA

Han Wang
The University of Kansas
Lawrence, USA

Ayesha Samreen
Iowa State University
Ames, USA

Christopher J. Quinn
Iowa State University
Ames, USA

Yan Yan
University of Illinois at Chicago
Chicago, USA

Ashish Kundu
Cisco Research
San Jose, USA

Yuan Hong
University of Connecticut
Storrs, USA

Abstract

Differentially Private Stochastic Gradient Descent (DP-SGD) is a standard method for enforcing privacy in deep learning, typically using the Gaussian mechanism to perturb gradient updates. However, conventional mechanisms such as Gaussian and Laplacian noise are parameterized only by variance or scale. This single degree of freedom ties the magnitude of noise directly to both privacy loss and utility degradation, preventing independent control of these two factors. The problem becomes more pronounced when the number of composition rounds T and batch size B vary across tasks, as these variations induce task-dependent shifts in the privacy-utility trade-off, where small changes in noise parameters can disproportionately affect model accuracy. To address this limitation, we introduce PLRV-O, a framework that defines a broad search space of parameterized DP-SGD noise distributions, where privacy loss *moments* are tightly characterized yet can be optimized more independently with respect to utility loss. This formulation enables systematic adaptation of noise to task-specific requirements, including (i) model size, (ii) training duration, (iii) batch sampling strategies, and (iv) clipping thresholds under both training and fine-tuning settings. Empirical results demonstrate that PLRV-O substantially improves utility under strict privacy constraints. On CIFAR-10, a fine-tuned ViT achieves 94.03% accuracy at $\epsilon \approx 0.5$, compared to 83.93% with Gaussian noise. On SST-2, RoBERTa-large reaches 92.20% accuracy at $\epsilon \approx 0.2$, versus 50.25% with Gaussian.¹

CCS Concepts

• Security and privacy; • Computing methodologies → Machine learning;

*Both authors contributed equally to this work.

¹Source code is available at <https://github.com/datasec-lab/plrvo>. This is the full version of the paper to appear in CCS'25.



This work is licensed under a Creative Commons Attribution 4.0 International License. CCS '25, Taipei, Taiwan

© 2025 Copyright held by the owner/author(s).
ACM ISBN 979-8-4007-1525-9/2025/10
<https://doi.org/10.1145/3719027.3765151>

Keywords

Differential Privacy, Deep Learning, Mechanism Design, Randomization, Optimization, Privately Fine-tuning Vision Transformer and Language Models

ACM Reference Format:

Qin Yang, Nicholas Stout, Meisam Mohammady, Han Wang, Ayesha Samreen, Christopher J. Quinn, Yan Yan, Ashish Kundu, and Yuan Hong. 2025. PLRV-O: Advancing Differentially Private Deep Learning via Privacy Loss Random Variable Optimization. In *Proceedings of the 2025 ACM SIGSAC Conference on Computer and Communications Security (CCS '25)*, October 13–17, 2025, Taipei, Taiwan. ACM, New York, NY, USA, 23 pages. <https://doi.org/10.1145/3719027.3765151>

1 Introduction

Training and fine-tuning deep learning models pose significant privacy risks. During training, adversaries can exploit gradient updates, model outputs, and pre-trained parameters to reconstruct sensitive data, making privacy a critical concern [66]. Moreover, fine-tuning large pre-trained language models, such as BERT [40] and GPT families [63], is essential for achieving state-of-the-art performance in various tasks, including sentence classification [40], text generation [46], and code generation [59]. Data reconstruction attacks, such as Updates-Leak [50] and Inverting Gradients [24], achieve success rates of up to 80%, while the Dynamic Memory Model Inversion Attack (DMMIA) [49] enhances realism, reaching 93.54% on FaceScrub; in the same line of work, Carlini et al. [12] demonstrate that Large Language Models (LLMs) can memorize and regurgitate up to 1.6% of training tokens verbatim. Additionally, prompt-based techniques further expose LLMs to data extraction attacks, increasing the risk of recovering individual samples.

To mitigate privacy risks during model training and fine-tuning, Differentially Private Stochastic Gradient Descent (DP-SGD) [1, 13, 16, 24] is widely used. DP-SGD applies the Gaussian mechanism [19], which preserves privacy by clipping gradients and adding Gaussian noise, protecting the membership status of individual samples in the model parameters. Additionally, DP-SGD bounds cumulative privacy leakage over thousands of training or fine-tuning steps by tightly analyzing the Privacy Loss Random

Table 1: Comparison of Gaussian, Laplace, and PLRV-O. Gaussian cannot reach high accuracy in high-privacy regimes (strong DP). Laplace cannot support subsampling accounting for privacy amplification, large models, or ℓ_2 clipping. Both mechanisms also lack the ability to optimize their randomization for the best privacy-utility tradeoff. Large Moments indicates support for higher-order Rényi DP moments, which improves utility in tight privacy accounting.

Mechanisms	Optimizing Noise	High Acc@Strong DP	Large Moments	Subsampling	Small Model	Large Model	ℓ_2 Clip.
Gaussian	✗	✗	✗	✓	✓	✓	✓
Laplace	✗	✗	✗	✗	✓	✗	✗
PLRV-O (ours)	✓	✓	✓	✓	✓	✓	✓

Variable (PLRV) of the Gaussian mechanism. However, DP-SGD often incurs significant accuracy loss, primarily due to the magnitude of the Gaussian noise, or “noise multiplier” (σ).²

Motivation. Existing DP-SGD solutions face significant limitations, and it is desirable to design a more sophisticated class of techniques.

First, DP-SGD using Gaussian noise offers limited flexibility in the achievable noise multiplier due to fundamental constraints. Gaussian noise faces intrinsic challenges in high-privacy regimes due to its $\sigma = \Theta(1/\epsilon)$ behavior [3]. Also, Mironov et al. [42] and Sander et al. [42, 51] identify the “privacy wall” phenomenon, where Gaussian noise fails to efficiently leverage higher DP moment orders (λ), leading to overestimation in privacy accounting [3]. This occurs because the PLRV of the Gaussian mechanism causes the Moments Accounting Function (MAF) to grow rapidly with λ due to its light-tailed behavior. Interestingly, Balle et al. [3] show that although $\sigma = \Theta(1/\epsilon)$ may help in low-privacy regimes (e.g., $\epsilon > 1$), the effect does not persist: the noise scale instead decreases proportionally to $1/\sqrt{\epsilon}$, leading to continued overcharging in privacy accounting even when looser privacy guarantees are acceptable.

Second, the Laplace mechanism [29] offers a PLRV with an exponentially heavier tail, allowing it to more efficiently leverage higher DP moment orders (λ) to tighten the accounted privacy budget.³ However, this advantage has not been fully realized in practice due to the challenges introduced by ℓ_1 -norm clipping in high-dimensional spaces (*DP-SGD with the Laplace mechanism requires ℓ_1 -norm clipping by default*). Specifically, for an n -dimensional gradient vector, the ℓ_1 norm can be up to \sqrt{n} times larger than the ℓ_2 norm. As a result, setting a clipping threshold C based on ℓ_2 -norm bounds would translate to an effective threshold of approximately $C \times \sqrt{n}$ in ℓ_1 -norm, rendering the resulting DP guarantees unbearably loose. On the other hand, using a smaller threshold to clip directly in ℓ_1 -norm quickly collapses the gradient space, severely harming model trainability and often making training impossible.

Third, the privacy-utility trade-off is heavily influenced by task-specific factors such as the number of epochs (E) and batch size (B), which directly affect privacy accounting through their role in the moments accounting function and subsampling amplification. Whether a task involves training or fine-tuning also shapes the trade-off space. For instance, DP-SGD with a smaller clipping threshold ($C \approx 0.1$) is often sufficient for fine-tuning large models, whereas training typically requires a larger clipping threshold. Each case leads to a radically different privacy-utility trade-off. Effectively leveraging these variations within the noise Probability Density Function (PDF) demands a more versatile class of DP-SGD

noise mechanisms, as opposed to traditional single-parameter approaches like Gaussian and Laplacian noise.

The PLRV-O Approach. To our knowledge, this work is the first to introduce the Privacy Loss Random Variable Optimization (PLRV-O) framework for noise design in DP-SGD. Unlike conventional single-parameter mechanisms, PLRV-O defines a structured search space of *randomized-scale Laplace* distributions, where privacy loss moments are tightly characterized and directly optimizable through the parameters of the scale distribution. This construction enables systematic exploration of diverse privacy-utility trade-offs under rigorous DP guarantees. Table 1 provides a comparison of PLRV-O with existing DP noise mechanisms used in DP-SGD.

PLRV-O for Vision and Language Models. PLRV-O is a generalized DP framework applicable to both model training and fine-tuning. In our evaluations, we instantiate it on vision tasks (training from scratch) and on large language models (fine-tuning). By replacing Gaussian noise in state-of-the-art methods with optimized noise distributions from PLRV-O, we enable more efficient use of the privacy budget and consistently improve model utility across diverse architectures, including ResNet, ViT, BERT, and RoBERTa [15, 40, 57]. Orthogonal techniques such as Ghost Clipping [39] can also be combined with PLRV-O, though their integration lies beyond the scope of this work. Therefore, our primary contributions are summarized below.

- (1) We propose PLRV-O, the first DP-SGD framework with an optimizable non-Gaussian noise mechanism. It defines a search space of PDFs with randomized scale parameters governed by a Gamma distribution, where varying the shape and scale enables systematic exploration of privacy-utility trade-offs. Privacy guarantees are tightly accounted for, ensuring rigorous bounds while adapting to task-specific objectives.
- (2) We introduce a theoretical advancement by applying Schur-convexity and majorization theory [52] to extend the Laplace family to the ℓ_2 metric, avoiding ℓ_1 clipping. This leads to a tight upper bound for the moments accountant, enabling more accurate privacy accounting and faster DP training.
- (3) We conduct comprehensive experiments across a diverse range of tasks in both computer vision (CV) and natural language processing (NLP), covering both training and fine-tuning, to validate our PLRV-O mechanism. The results demonstrate PLRV-O’s effectiveness across various tasks, showing improved privacy-utility trade-offs over SOTA methods, especially in the stronger privacy regime ($0 < \epsilon < 1$).

2 Preliminaries

We review some background on differential privacy and DP-SGD for the theoretical foundations of the PLRV-O framework.

²In DP-SGD, gradient clipping primarily impacts training stability, as overly aggressive thresholds can render models untrainable [1, 3, 27].

³Earlier work on query answering under DP shows that the Laplace mechanism can preserve accuracy better than the Gaussian mechanism in stricter privacy regimes, particularly in low-dimensional settings [26, 43].

2.1 Differential Privacy

Differential privacy protects data privacy by introducing randomness into the output, either by injecting explicit noise or by leveraging inherent stochasticity in the mechanism or inputs⁴. Let \mathcal{D} be the space of datasets. For a query $q : \mathcal{D} \rightarrow \mathbb{R}^n$, we denote by $M_q : \mathcal{D} \times \Omega \rightarrow \mathbb{R}^n$ the randomized mechanism answering q . We say that two datasets $d, d' \in \mathcal{D}$ are *adjacent*, written $\text{Adj}(d, d')$, if they differ in the data of exactly one participant.

Definition 2.1 (Differential Privacy). A mechanism M_q satisfies ϵ -DP if, for all adjacent $d, d' \in \mathcal{D}$ and all measurable $S \subseteq \mathbb{R}^n$:

$$\Pr[M_q(d) \in S] \leq e^\epsilon \Pr[M_q(d') \in S].$$

If the inequality fails, an ϵ -breach occurs, indicating a non-negligible difference between the prior and posterior distributions. We next recall the Laplace Mechanism [17], a fundamental tool for achieving ϵ -differential privacy. Recall that the (univariate) Laplace distribution with mean zero and scale b , denoted $\text{Lap}(b)$, has density $p(x; b) = \frac{1}{2b} \exp(-|x|/b)$ and variance $2b^2$. For $w \in \mathbb{R}^n$ with i.i.d. components $w_i \sim \text{Lap}(b)$, the joint density is $(\frac{1}{2b})^n \exp(-\|w\|_1/b)$ and $\|\cdot\|_1$ denotes the ℓ_1 norm [58].

Definition 2.2 (Laplace Mechanism). Given a numerical query $q(d)$ and a scale b , the Laplace mechanism $M_q(d, b)$ modifies $q(d)$ by adding noise $z \sim \text{Lap}(b)$, i.e., $M_q(d, b) = q(d) + z$.

The scale parameter in the Laplace mechanism controls the level of privacy. Specifically:

THEOREM 2.3. Let $q : \mathcal{D} \rightarrow \mathbb{R}$ be a query with (global) ℓ_1 -sensitivity $\Delta_1 q = \max_{d, d' : \text{Adj}(d, d')} \|q(d) - q(d')\|_1$. If the Laplace mechanism $M_q(d, b)$ uses a scale parameter $b \geq \frac{\Delta_1 q}{\epsilon}$, then $M_q(d, b)$ is ϵ -differentially private.

After the original definition of pure DP [17], approximate DP was introduced to account for Gaussian noise, adding a δ typically on the order of $1/|\mathcal{D}|$, that represents the probability of violating the ϵ -DP guarantee [18].

Definition 2.4 (Approximate Differential Privacy). A randomization mechanism $M_q : \mathcal{D} \rightarrow \mathcal{R}$ is said to provide (ϵ, δ) -differential privacy for releasing the query results $q(\mathcal{D})$ if it randomizes its output such that, for any two adjacent datasets $d, d' \in \mathcal{D}$ and all subset $S \subseteq \mathbb{R}^n$, the following holds:

$$\Pr[M_q(d) \in S] \leq e^\epsilon \Pr[M_q(d') \in S] + \delta. \quad (1)$$

The Gaussian mechanism, described below, achieves approximate (ϵ, δ) -differential privacy [18].

Definition 2.5 (Gaussian Mechanism). The Gaussian mechanism $M_q(d, \sigma)$ modifies the answers to query q in the dataset d by adding noise $z \sim \mathcal{N}(0, \sigma^2 I)$, that is, $M_q(d, \sigma) = q(d) + z$.

In particular, for $\epsilon < 1$, its standard deviation is given by $\sigma = \frac{\Delta_2 q}{\epsilon} \sqrt{2 \ln(\frac{1.25}{\delta})}$, where $\Delta_2 q$ is the ℓ_2 -sensitivity of the query q across all adjacent datasets.

⁴Developing a unified framework to capture all randomness sources and translate them into differential privacy guarantees remains an open challenge [42]. Here, we assume a fixed probability space (Ω, \mathcal{F}, P) , where Ω is the sample space, \mathcal{F} is a σ -algebra of events, and P is the probability measure.

Sequentially applying DP mechanisms increases the overall privacy cost, as shown by various composition theorems [20, 22, 36]. Naïve composition states that chaining k mechanisms, each (ϵ, δ) -DP, results in an overall $(k\epsilon, k\delta)$ -DP guarantee, which can be overly conservative. Stronger composition theorems, such as the *advanced composition* theorem [35], provide tighter bounds. In particular, the overall DP guarantee can become $(\epsilon \sqrt{2k \ln(\frac{1}{\delta})} + k\epsilon(\epsilon - 1))$.

2.2 Deep Learning with Differential Privacy

DP-SGD [1] was the first method to incorporate DP into deep neural network (DNN) training. At each iteration t , the gradient $\mathbf{g}_t(\mathbf{x}_i)$ for a data point \mathbf{x}_i is clipped using a threshold C . Formally, the clipped variant of gradients is given by $\bar{\mathbf{g}}_t(\mathbf{x}_i) = \mathbf{g}_t(\mathbf{x}_i) / \max(1, \frac{\|\mathbf{g}_t(\mathbf{x}_i)\|_2}{C})$. This limits the sensitivity of each gradient, preparing it for the Gaussian mechanism, yielding “sanitized” gradients for all $1 \leq i \leq n$

$$\mathbf{g}_t^s(\mathbf{x}_i) = \bar{\mathbf{g}}_t(\mathbf{x}_i) + \mathbf{z}, \quad (2)$$

where $\mathbf{z} \sim \mathcal{N}(0, C^2 \sigma^2 \mathbf{I}_n)$. The final update $\bar{\mathbf{g}}_t^s$ is computed by averaging $\mathbf{g}_t^s(\mathbf{x}_i)$ over the batch of size B . Even with tighter composition bounds, training over many iterations (e.g., thousands of rounds) can lead to high cumulative privacy loss (ϵ). DP-SGD mitigates this by formulating an accounting function over the privacy loss terms across rounds, namely the *Moments Accountant Function*. Consequently, DP-SGD with moments accounting achieves a significantly improved bound of $O(\epsilon \sqrt{TB}/|d|, \delta)$ -DP.

2.2.1 Moments Accounting Function. Consider two neighboring datasets $d, d' \in \mathcal{D}$ and an outcome $o \in \mathbb{R}^n$ from the minibatch average $\bar{\mathbf{g}}_t^s$ of sanitized gradients. The *privacy loss* associated with o is defined by

$$c(o; \text{aux}, d, d') = \log \frac{\Pr[\bar{\mathbf{g}}_t^s(\text{aux}, d) = o]}{\Pr[\bar{\mathbf{g}}_t^s(\text{aux}, d') = o]}. \quad (3)$$

where “aux” represents any state accumulated over sequential DP mechanisms. Since $\bar{\mathbf{g}}_t^s(\cdot)$ is randomized, $c(o; \text{aux}, d, d')$ is itself a random variable. To bound privacy loss more tightly, the moments of the random variable associated with $c(o; \text{aux}, d, d')$ are tightly calculated and bounded. Precisely, for $\lambda > 0$, define

$$\alpha_{\bar{\mathbf{g}}_t^s}(\lambda; \text{aux}, d, d') = \log \mathbb{E}_{o \sim \bar{\mathbf{g}}_t^s(\text{aux}, d)} [\exp(\lambda c(o; \text{aux}, d, d'))]. \quad (4)$$

We then take the worst-case value over aux, d, d' :

$$\alpha_{\bar{\mathbf{g}}_t^s}(\lambda) = \max_{\text{aux}, d, d'} (\alpha_{\bar{\mathbf{g}}_t^s}(\lambda; \text{aux}, d, d')). \quad (5)$$

Key properties of this *Moments Accountant Function (MAF)* include:

- (1) **Composability.** For a sequence of adaptive mechanisms $\bar{\mathbf{g}}_1^s, \dots, \bar{\mathbf{g}}_t^s$,

$$\alpha_{\bar{\mathbf{g}}_1^s, \dots, \bar{\mathbf{g}}_t^s}(\lambda) \leq \sum_{i=1}^t \alpha_{\bar{\mathbf{g}}_i^s}(\lambda). \quad (6)$$

- (2) **Tail Bound.** For any $\epsilon > 0$, releasing $\bar{\mathbf{g}}_1^s, \dots, \bar{\mathbf{g}}_t^s$ is (ϵ, δ) -DP if

$$\delta = \min_{\lambda > 0} (\exp(\alpha_{\bar{\mathbf{g}}_1^s, \dots, \bar{\mathbf{g}}_t^s}(\lambda)) - \lambda \epsilon). \quad (7)$$

2.2.2 Privacy Amplification with Subsampling. While the Moments Accountant (MAF) significantly tightens the privacy budget, DP-SGD’s main strength arises from *privacy amplification via random sampling*, where the privacy cost per evaluation decreases *quadratically*—rather than linearly—with the sampling rate $\zeta = \frac{B}{|\mathcal{D}|}$. For instance, Bun et al. [9] show that $\alpha(\lambda) \propto \zeta^2 \frac{6\lambda}{\sigma^2}$. Mironov et al. [42] (Section 3.3) presented a tighter privacy amplification bound, which remains the state-of-the-art for the subsampled Gaussian mechanism. The bound is expressed as:

$$\alpha_{\mathbf{g}_1^s, \dots, \mathbf{g}_t^s}(\lambda) \leq t \log \left[\sum_{\eta=0}^{\lambda+1} \binom{\lambda+1}{\eta} (1-\zeta)^{\lambda+1-\eta} \zeta^\eta \exp \left(\frac{\eta^2 - \eta}{2\sigma^2} \right) \right]. \quad (8)$$

The final (ϵ, δ) -DP guarantee is derived using the tight conversion formula provided by Balle et al. [2], which holds for any mechanism, by substituting in the moment bounds $\alpha_{\mathbf{g}_1^s, \dots, \mathbf{g}_t^s}(\lambda)$ for $\alpha(\lambda)$:

$$\epsilon(\delta) = \min_{\lambda > 0} \left(\frac{\alpha(\lambda)}{\lambda} + \log \left(\frac{\lambda}{\lambda+1} \right) - \frac{\log(\delta) + \log(\lambda+1)}{\lambda} \right). \quad (9)$$

This formulation significantly enhances the analysis of privacy loss in scenarios involving repeated subsampling and Gaussian noise.

3 Problem Statement

Let Θ denote the noise in DP-SGD, and let X denote a set of fixed or tunable learning parameters under consideration. Specifically, we may take $X = (E, B, C, n)$, where E is the number of training epochs, B is the batch size, C is the clipping threshold, and n is the number of model parameters. Note that the pair (E, B) can equivalently be represented by the **total number of rounds** T and the **sample rate** $\zeta = \frac{B}{N}$, where N is the dataset size, since $T = \lceil \frac{E \cdot N}{B} \rceil$. The learning rate lr and the initial state (random initialization or pre-trained weights for fine-tuning) are additional training parameters, but they are not part of our optimization problem.

Define $\epsilon(X, \Theta, \delta)$ as the privacy budget achieved by Θ under parameters X and target DP failure probability δ . We denote by $U(X, \Theta)$ the user’s chosen utility function, which measures task-specific performance at the end of training/fine-tuning with DP-SGD noise parameters Θ and learning parameters X for a given initial neural network, dataset, and loss function. Given fixed learning parameters $X = (E, B, C, n)$, our objective is to design the noise distribution (i.e., select PDF for optimal noise Θ^*) that maximizes the utility subject to a constraint on privacy budget:

$$\max_{\Theta} U(X, \Theta^*) \quad \text{subject to} \quad \epsilon(X, \Theta, \delta^*) \leq \epsilon^*. \quad (10)$$

3.1 Optimizing Gaussian DP-SGD

In practice, the utility U lacks an analytic form⁵ and does not admit provable numerical optimization, offering only zeroth-order feedback (i.e., observable outputs without derivative information) after E epochs of training/fine-tuning and then model evaluation with respect to U . Likewise, the privacy budget $\epsilon(X, \Theta, \delta^*)$ in general does not have a known expression, though analytic upper-bounds on privacy loss may be known. Consequently, because solving Equation (10) is intractable, a common alternative is to optimize a

⁵Even if the utility is a loss function that is differentiable with respect to the model parameters, the loss at the end of training/fine-tuning’s dependence on DP-SGD noise parameters would not have a (known) analytic form.

surrogate utility function, such as the noise multiplier, after carefully setting the clipping threshold C . If C is too small, nearly all gradients are clipped, leading to an insufficient signal-to-noise ratio (SNR) and preventing convergence. Conversely, if C is too large, the effective noise scale in Gaussian DP-SGD ($C\sigma$) becomes excessive, which degrades model utility.

Signal to Noise Ratio: The interaction between clipping and noise variance directly impacts learning performance, and prior work has explored optimizing the clipping value C . Importantly, C cannot be set arbitrarily small, as this prevents effective learning. While very small clipping values (e.g. 0.1) have been shown to work for fine-tuning large pre-trained models [39], pre-training tasks typically require much larger thresholds, in the range of 3–20 [1]. Thus, the surrogate optimization problem becomes

$$\min_{\sigma > 0} \sigma \quad \text{subject to} \quad \epsilon(X, \Theta, \delta^*) \leq \epsilon^*,$$

where X implicitly assumes the task-specific minimal clipping value C^* . Using the privacy loss upper bound Equation (9) in place of $\epsilon(X, \Theta, \delta^*)$, the optimization in Equation (3.1) reduces to a simple trade-off: larger σ yields a smaller privacy budget ϵ , and vice versa. Exploiting this monotonic relationship, we can then perform a simple numerical search to identify the smallest feasible σ^* such that $\epsilon(\delta) < \epsilon^*$.

Going beyond the Gaussian case, we define a generic distortion measure to capture the effect of noise. Let $\mathbb{P}_{\Theta}(x)$ denote the PDF of a noise distribution parameterized by Θ , where x represents the noise sample value. The ℓ_1 error, or distortion, of a noise distribution is defined as

$$\text{Distortion}(\Theta) = \int |x| \mathbb{P}_{\Theta}(x) dx.$$

For instance, this expression for Gaussian noise is $\sigma \sqrt{\frac{2}{\pi}}$. The corresponding optimization problem is

$$\min_{\Theta} \text{Distortion}(\Theta) \quad \text{subject to} \quad \epsilon(X, \Theta, \delta^*) \leq \epsilon^*. \quad (11)$$

3.2 Drawbacks of Gaussian and Laplace Noise

Optimizing over σ alone has critical limitations with a single decision variable, which simultaneously controls both utility and privacy. This coupling is inherently limiting: with only one degree of freedom, optimizing for one objective (utility or privacy) directly impacts the other.

First, the standard delta test, $\delta(\epsilon \rightarrow 0)$, provided by Balle et al. in [2], is an asymptotic test that demonstrates the failure probability δ of the Gaussian mechanism performs nearly 100 times worse than that of the Laplace mechanism in high-privacy regimes. Figure 1 shows the ratio between the delta tests for Gaussian and Laplace mechanisms, highlighting the increased cost of using Gaussian noise to achieve stronger protection. This inflated δ in high-privacy regimes directly increases the accounted budget $\epsilon(\delta)$ through the $-\log(\delta)$ term in the tight conversion formula Equation (9). The limitation stems from the light tail of the Gaussian PDF, with its quadratic exponential decay. By contrast, the Laplace distribution, with heavier tails, is known to be optimal as $\epsilon \rightarrow 0$ under ℓ_1 and ℓ_2 mean error for scalar queries [26].

However, Laplace introduces its own challenges for DP-SGD, particularly requiring ℓ_1 -norm clipping, which severely degrades

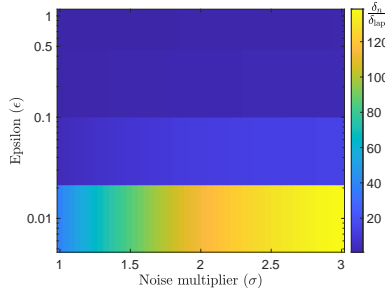


Figure 1: Delta test ratio $\delta(\epsilon \rightarrow 0)$ of the Gaussian to Laplace mechanisms under varying noise levels. Laplace mechanism significantly outperforms Gaussian in $\epsilon \rightarrow 0$.

performance in high-dimensional spaces. Recall the relationship $\|x\|_1 \leq \sqrt{n}\|x\|_2$, a direct consequence of the Cauchy–Schwarz inequality [55]. The volumes of clipped spaces—the ℓ_1 cross-polytope and ℓ_2 ball—scale as $V_{\ell_1}(n, C) = \frac{(2C)^n}{n!}$ and $V_{\ell_2}(n, C) = \frac{\pi^{n/2} C^n}{\Gamma(n/2 + 1)}$, respectively, with their ratio $\frac{V_{\ell_1}(n, C)}{V_{\ell_2}(n, C)} = \left(\frac{2}{\sqrt{\pi}}\right)^n \frac{(\frac{n}{2})!}{n!}$ shrinking exponentially in n . As shown in Figure 2, ℓ_1 clipping rapidly becomes restrictive, discarding far more gradients than ℓ_2 clipping. This likely explains why Laplace mechanisms are rarely used in DP-SGD, as retaining sufficient learning capacity under ℓ_1 clipping requires inflating the noise by a factor proportional to \sqrt{n} , i.e., the noise must grow with the model size.

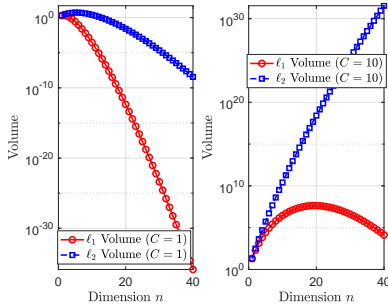


Figure 2: The volume of n -dimensional vector space clipped by C - ℓ_1 and C - ℓ_2 norms.

Second, task-specific DP-SGD optimization requires a much larger decision space than Gaussian or Laplace mechanisms, which each rely on a single parameter (variance σ^2 or $2b^2$). Factors such as epochs (E), batch size (B), and whether the task is fine-tuning or pretraining directly shape privacy accounting and clipping needs, producing very different privacy–utility trade-offs. This nonlinearity calls for noise mechanisms more versatile than Gaussian or Laplace. An ideal mechanism would (i) combine their strengths and (ii) introduce free parameters in its standard deviation to flexibly balance (ϵ, δ) -DP guarantees with task-specific accuracy.

4 Methodology

4.1 ℓ_2 Clipping over Laplace’s Privacy Loss

Recall that the Laplace mechanism faces limitations with ℓ_1 clipping, while Gaussian noise exhibits the “privacy wall” phenomenon. To address these issues and move toward a mechanism that combines

the strengths of both, we first characterize the privacy loss of the Laplace mechanism (proof in Appendix B.1) and then define the resulting challenges and an effective solution.

THEOREM 4.1 (PRIVACY LOSS OF A LAPLACE MECHANISM). *The privacy loss of a Laplace mechanism with scale parameter b , applied to gradients clipped by C under the ℓ_1 norm, is bounded as:*

$$c(o; \text{aux}, d, d', b) \leq \frac{C}{b}. \quad (12)$$

Since this bound is tight for the Laplace mechanism [19], DP-SGD with Laplace noise inherently requires scaling the noise with the ℓ_1 norm of the n -dimensional clipped gradient. Given any required ℓ_2 -clipped gradient space—for example, $C \geq 0.1$ in fine-tuning tasks—the ratio $\frac{\ell_1}{\ell_2} \leq \sqrt{n}$ causes the effective ℓ_1 clipping threshold to grow rapidly with n , forcing C to become very large.

We will later propose an alternative approach that applies ℓ_2 clipping to gradients and computes the moments accountant function (MAF) separately for each model parameter, composing the results across all parameters. This strategy will be motivated by the following behavior of the MAF for univariate Laplace mechanisms (e.g., using ℓ_1 clipping), which allows us to leverage a much larger number of privacy loss moments λ than with the Gaussian mechanism (on the order of thousands) when analyzing a single query. See Appendix B.2 for the proof.

THEOREM 4.2 (SUBSAMPLED UNIVARIATE LAPLACE MECHANISMS). *Let M be a univariate Laplace mechanism with scale parameter b and sampling probability $\zeta = \frac{L}{N}$, where L is the mini-batch size and N is the dataset size. Suppose M is applied to a single partial derivative query (i.e., with respect to a single model parameter) $q(d) = g(d)$ clipped by threshold C , i.e., $|g| \leq C$.*

Then, the moments accountant function of M_q satisfies

$$\alpha_{M_q}(\lambda) = \log \left[\sum_{\eta=0}^{\lambda+1} \binom{\lambda+1}{\eta} (1-\zeta)^{\lambda+1-\eta} \zeta^\eta F(C, \eta) \right], \quad (13)$$

where

$$F(C, \eta) = \frac{\eta e^{\frac{(\eta-1)C}{b}} + (\eta-1)e^{-\frac{\eta C}{b}}}{2\eta-1}. \quad (14)$$

While the univariate analysis in Equation (13) provides an exact expression for each parameter, directly summing over millions of parameters can still lead to significant overestimation of the total privacy loss unless a tight holistic (multivariate) bound is applied.⁶

To address this overestimation, we apply *Majorization Theory* [41, 56], a powerful tool for comparing vectors based on their spread or concentration. After ℓ_2 clipping with threshold C , the marginal clipped gradients $|g_i|$ are mostly small but unevenly distributed. To capture this structure, we construct a *majorization set*—a specially ordered vector that dominates the original gradient vector.

This majorization set enables us to bound any Schur-convex function of the original gradients by its value on the majorization set. Since the MAF depends on the gradients through a Schur-convex structure, applying majorization allows us to obtain a tight holistic (multivariate) privacy bound for ℓ_2 -clipped gradients.

⁶Here, the summation is over model parameters rather than training/fine-tuning iterations, similar to how composability traditionally applies over iterations. For the overall training/fine-tuning process, we would also need to compose over iterations.

In what follows, we first introduce background on majorization theory, then show that the moments accountant function given in Equation (13) is Schur-convex. Finally, we derive a tight majorization set and use it to bound the total moment accountant function for Laplace mechanisms.

4.1.1 Majorization Theory Background. For two vectors $\mathbf{x}, \mathbf{y} \in \mathbb{R}^n$, we say that \mathbf{x} *weakly majorizes* \mathbf{y} from below, denoted $\mathbf{x} \succ_w \mathbf{y}$, if the following condition holds:

$$\sum_{i=1}^k x_i^\downarrow \geq \sum_{i=1}^k y_i^\downarrow \quad \text{for all } k = 1, \dots, n,$$

where x_i^\downarrow and y_i^\downarrow denote the i -th largest components of \mathbf{x} and \mathbf{y} , respectively [41, 56]. That is, both vectors are assumed to be sorted in non-increasing order before comparison.

A function $F : \mathbb{R}^n \rightarrow \mathbb{R}$ is called *Schur-convex* if $\mathbf{x} \prec \mathbf{y} \Rightarrow F(\mathbf{x}) \leq F(\mathbf{y})$. Intuitively, Schur-convex functions favor vectors that are more “spread out,” making them useful for bounding symmetric functionals.

Schur–Ostrowski Criterion [48]. Let $f : \mathbb{R}^d \rightarrow \mathbb{R}$ be a symmetric function with continuously differentiable partial derivatives. Then f is Schur-convex if and only if for all $\mathbf{x} \in \mathbb{R}^d$ and for all $1 \leq i, j \leq d$, the following inequality holds:

$$(x_i - x_j) \left(\frac{\partial f}{\partial x_i} - \frac{\partial f}{\partial x_j} \right) \geq 0.$$

The following result is proven in Appendix B.3.

THEOREM 4.3 (SCHUR-CONVEXITY OF MAF). Let $\tilde{\mathbf{G}} = \{\tilde{\mathbf{g}}_1, \dots, \tilde{\mathbf{g}}_n\}$ be the set of differentially private gradients obtained by applying ℓ_2 clipping followed by a multivariate Laplace mechanism. Let $\alpha_{\tilde{\mathbf{g}}_i}(\lambda)$ denote the moment accountant function for coordinate i .

Then, the total moment accountant function

$$\alpha_{\tilde{\mathbf{G}}}(\lambda) = \sum_{i=1}^n \alpha_{\tilde{\mathbf{g}}_i}(\lambda) \quad (15)$$

is **Schur-convex** with respect to the marginal clipped gradients $|\mathbf{g}_i|$.

With $\alpha(\lambda)$ being Schur-convex, we now introduce a majorization set over \mathbf{G} , the ℓ_2 clipped (but not noisy) gradient vector. The following result is proven in Appendix B.4.

LEMMA 4.4 (MAJORIZATION SET CONSTRUCTION). Let $\mathbf{G} = \{\mathbf{g}_1, \dots, \mathbf{g}_n\}$ be the marginal clipped gradients sorted in descending order. Then, $|\mathbf{G}|$ is weakly majorized by the vector $\mathbf{x} = \{x_1, \dots, x_n\}$ defined by

$$x_i = C \left(\sqrt{i} - \sqrt{i-1} \right), \quad i = 1, \dots, n,$$

where C is the ℓ_2 clipping threshold. That is,

$$|\mathbf{G}| \prec_w \mathbf{x},$$

where \prec_w denotes the weak majorization order.

We now extend the univariate moments accountant to the multivariate setting by summing across coordinates, where each coordinate i uses its corresponding majorization bound x_i . The following theorem naturally follows from Theorems 4.2, 4.3, and Lemma 4.4.

THEOREM 4.5 (SUBSAMPLED MULTIVARIATE LAPLACE MECHANISM). Let $\tilde{\mathbf{G}} = \{\tilde{\mathbf{g}}_1, \dots, \tilde{\mathbf{g}}_n\}$ be the set of differentially private gradients obtained by applying C - ℓ_2 clipping followed by a multivariate Laplace mechanism with scale b and sampling probability ζ . Define the majorization set $\mathbf{x} = \{x_1, \dots, x_n\}$ by

$$x_i = C \left(\sqrt{i} - \sqrt{i-1} \right), \quad i = 1, \dots, n.$$

Then, the total moment accountant satisfies

$$\alpha_{\tilde{\mathbf{G}}}(\lambda) \leq \sum_{i=1}^n \log \left[\sum_{\eta=0}^{\lambda+1} \binom{\lambda+1}{\eta} (1-\zeta)^{\lambda+1-\eta} \zeta^\eta F(x_i, \eta) \right], \quad (16)$$

where

$$F(x_i, \eta) = \frac{\eta e^{\frac{(\eta-1)x_i}{b}} + (\eta-1)e^{-\frac{\eta x_i}{b}}}{2\eta - 1}. \quad (17)$$

4.2 DP-SGD Beyond Gaussian and Laplace

To address the second objective, we propose a new class of noise, namely *PLRV noise*, a randomized-scale extension of the standard Laplace mechanism. The scale parameter b is drawn from a non-negative probability density function $f : \mathbb{R}_{\geq 0} \rightarrow \mathbb{R}^+$, defined over the probability space (Ω, \mathcal{F}, P) . A PLRV noise is particularly notable for its ability to effectively **separate** accounting from distortion—using its scale PDF parameters. In the next section, we construct a search space of candidate PLRV distributions that can be efficiently optimized to guarantee very small privacy budgets.

Definition 4.6 (PLRV Noise). PLRV noise $z \in \mathbb{R}^n$ is drawn from a mixture of zero-mean multivariate Laplace distributions, where the scale b is randomized according to a non-negative density $f(b)$. Formally, its density is given by

$$p(z; f) = \int_{\mathbb{R}_{\geq 0}} f(b) \left(\frac{1}{2b} \right)^n \exp \left(-\frac{\|z\|_1}{b} \right) db, \quad (18)$$

with $\|z\|_1 = \sum_{i=1}^n |z_i|$ and f referred to as the PLRV seed.

Definition 4.7 (PLRV Mechanism). Let $q(d) \in \mathbb{R}^n$ be a numerical query and $z \sim p(z; f)$ be PLRV noise as defined in Equation (18). The PLRV mechanism is given by $M_q(d, f) = q(d) + z$.

Technically, DP-SGD with a PLRV mechanism involves a two-step sampling process: first, sampling a scale parameter, and second, using the sampled scale to generate noise from a zero-mean multivariate Laplace distribution.

Derived from the Laplace mechanism, the following exact moments accounting result is obtained by applying the law of total expectation to Theorem 4.2. The proof is in Appendix C.1.

THEOREM 4.8 (SUBSAMPLED UNIVARIATE PLRV MECHANISM). Let M_g be a univariate PLRV mechanism with scale $b \sim f(b)$, where f is a non-negative density. It is applied to a single partial derivative $g \in [-C, C]$, clipped at threshold C . Assume g is computed from a mini-batch sampled with probability $\zeta = \frac{1}{N}$, where L is the batch size and N is the dataset size. Define $u = 1/b$ and let $h(u) = \frac{1}{u^2} f\left(\frac{1}{u}\right)$ denote the density of the reciprocal scale. Then, the moments accounting function satisfies:

$$\alpha_{M_q}(\lambda) \leq \log \left\{ \sum_{\eta=0}^{\lambda+1} \binom{\lambda+1}{\eta} (1-\zeta)^{\lambda+1-\eta} \zeta^\eta \mathcal{G}(C, \eta) \right\},$$

where

$$\mathcal{G}(C, \eta) = \frac{\eta}{2\eta - 1} \mathcal{M}_u((\eta - 1)C) + \frac{\eta - 1}{2\eta - 1} \mathcal{M}_u(-\eta C).$$

\mathcal{M}_u denotes the moment generating function (MGF) for a random variable u . (see Appendix A for details). Using the majorization trick, the following bound is obtained.⁷

THEOREM 4.9 (MULTIVARIATE PLRV MECHANISM). *Let $\tilde{\mathbf{G}} = \{\tilde{\mathbf{g}}_1, \dots, \tilde{\mathbf{g}}_n\}$ be the set of differentially private gradients obtained by applying C - ℓ_2 clipping followed by a multivariate PLRV mechanism with scale $b \sim f(b)$, where f is a non-negative density. Define $u = 1/b$ and let $h(u) = \frac{1}{u^2} f(\frac{1}{u})$ be the density of the reciprocal scale. Then, the moments accounting function under subsampling probability ζ satisfies:*

$$\alpha_{\tilde{\mathbf{G}}}(\lambda) \leq \sum_{i=1}^n \log \left[\sum_{\eta=0}^{\lambda+1} \binom{\lambda+1}{\eta} (1-\zeta)^{\lambda+1-\eta} \zeta^\eta \mathcal{G}(x_i, \eta) \right], \quad (19)$$

where

$$\mathcal{G}(x_i, \eta) = \frac{\eta}{2\eta - 1} \mathcal{M}_u((\eta - 1)x_i) + \frac{\eta - 1}{2\eta - 1} \mathcal{M}_u(-\eta x_i). \quad (20)$$

The PLRV mechanism models seed distributions as linear combinations of non-negative random variables, enabling composable MGFs and a clean MAF bound via weighted log-MGF sums.

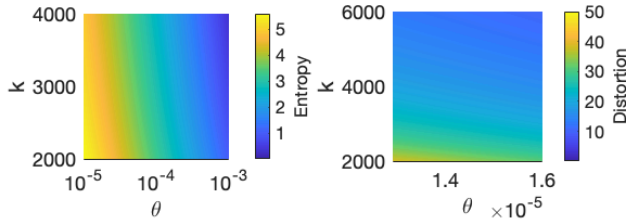


Figure 3: Visualization of θ controlling entropy (privacy, learnability) and k controlling distortion (accuracy).

Gamma-Distributed Seeds in PLRV. This composability enables flexible MAF dynamics optimized for learning parameters $X = (E, B, C)$ and privacy targets (ϵ, δ) . Positive-domain distributions with known MGFs—e.g., exponential, chi-squared, Weibull—can be combined to tailor noise for specific trade-offs. Among them, gamma distributions are especially effective due to their two-parameter flexibility and maximum entropy property (see Figure 3).⁸ We adopt this family, denoted Γ -PLRV, in the remainder of the paper.

Definition 4.10 (Γ -PLRV Noise). The Γ -PLRV noise is a specific instantiation of the PLRV noise, where the inverse scale parameter u follows a gamma distribution with shape parameter $k > 0$ and scale parameter $\theta > 0$. The resulting noise density is expressed as:

$$p(z; k, \theta) = \int_0^\infty \frac{b^{k-1} e^{-b/\theta}}{\theta^n \Gamma(k)} \left(\frac{1}{2b} \right)^n \exp \left(-\frac{\|z\|_1}{b} \right) db,$$

where $\Gamma(k)$ is the gamma function.

The Γ -PLRV class allows flexibility in adjusting the noise properties through k and θ .

⁷The Schur-convexity of the MAF for a PLRV mechanism (Theorem 4.8) follows directly from our earlier Laplace proof, as $\mathcal{G}(C, \eta)$ can be viewed as the expectation of $F(C, \eta)$.

⁸The gamma distribution maximizes entropy among distributions with fixed positive mean $E[X] = \alpha/\lambda$ and fixed $E[\ln X] = \psi(\alpha) - \ln \lambda$, where ψ is the digamma function [58].

5 The PLRV-O Framework

The PLRV-O framework (see Figure 4) enables task-specific optimization of DP training by adapting noise and clip parameters to the learning setup. The PLRV-O Kernel takes user-provided input $[T, \zeta, n, N, \epsilon^*, \delta^*]$ and searches for the optimal configuration (θ^*, k^*, C^*) using Algorithms 1 and 2. The selected noise and clip parameters are then applied in our PLRV-O DP-SGD (see Algorithm 3 in the Appendix). PLRV-O comprises three key modules:

(1) PLRV-O Search Space (SS). This module constructs a candidate set of PLRV-O configurations—triplets of shape k , scale θ , and clipping threshold C —from the user-specified training and privacy parameters $(T, \zeta, n, N, \epsilon^*, \delta^*)$. The result is a search space $\{(k, \theta, C)\}$, described in detail in Section 5.1, with alternative construction strategies discussed in Appendix D.2.

(2) ℓ_2 -Clipping (Majorization Set). This module generates a majorization set based on the model size and clipping parameter (in search space), thereby extending the ℓ_2 -clipping to the PLRV-O mechanism, as discussed in Section 4.1.1.

(3) Constrained Optimization. This module solves a constrained optimization problem to obtain the optimal (k^*, θ^*, C^*) . The *Moments Accounting* block (left-hand component) computes a tight upper bound on ϵ given δ for the PLRV-O mechanism. The *Distortion Minimization* block (right-hand component) filters the candidate search space to retain only configurations under a specified distortion threshold (e.g., distortion < 10). Both blocks jointly define the constraints for the optimization.

Algorithm 1 Constrained Optimization of PLRV-O Parameters

- 1: **Input:** Privacy budget $\epsilon(\delta)$, sampling rate ζ , steps T , max moment order λ_{\max} , convergence tol. τ , clip-span ratio $\rho \approx 2$
- 2: **Output:** (k^*, θ^*, C^*)
- // Phase I: determine a feasible clip range**
- 3: $C_{\min} \leftarrow$ SMALLEST C WITH ABOVE RANDOM ACCURACY AFTER A FEW EPOCHS
- 4: $C_{\max} \leftarrow \rho C_{\min}$ // experimentally, $\rho \approx 2$
- 5: $\mathbf{c}_0 : C_{\min} \leq C \leq C_{\max}$ // clip bounded search
- // Phase II: joint optimization over (k, θ, C)**
- 6: **Objective:** $J(k, \theta, C) = C(k - 1)\theta$
- // Constraints**
- 7: $\mathbf{c}_1 : \text{GammaCDF}(0.1; k, \theta) \approx 0$ // avoids unstable large- b regimes
- 8: $\mathbf{c}_2 : \epsilon(\delta) \leftarrow \text{MAF_PLRV-O}(k, \theta, \zeta, T, C, \delta)$ // privacy budget match
- 9: $\mathbf{c}_3 : k > 1$ // ensures finite expected ℓ_1 -error
- 10: $\mathbf{c}_4 : \theta > \frac{0.1}{k-1}$ // caps distortion
- 11: **Solve:** $\max_{k, \theta, C} J(k, \theta, C)$ s.t. $\mathbf{c}_0 - \mathbf{c}_4$ // use a constrained nonlinear solver, e.g., fmincon
- 12: **return** (k^*, θ^*, C^*)

We now analyze the PLRV-O framework, showing that Algorithm 3 (in Appendix) solves Problem Equation (10) from Section 3.1.

5.1 Analysis: Formulating PLRV-O Constraints

Recent work on scaling laws for baseline Gaussian DP-SGD, e.g., Sander et al. [51], shows in a one-dimensional analysis that the signal-to-noise ratio (SNR) governs the privacy budget. In this view,

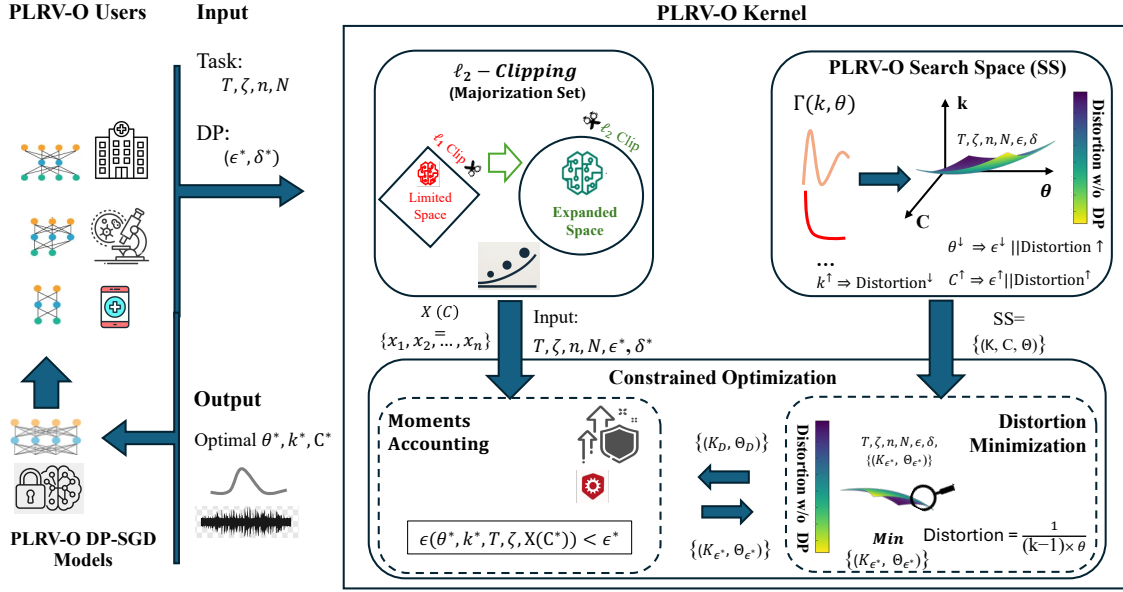


Figure 4: An overview of the PLRV-O framework.

Algorithm 2 PLRV-O Moments Accountant (MAF_PLRV-O)

Input: Moment $\lambda \in \mathbb{N}_+$, Sampling rate ζ , PLRV-O parameters (k, θ) , Population N , Clipping threshold C

Output: Order- λ log moment α_λ

```

1:  $n \leftarrow \lambda + 1$ 
2:  $\text{sum} \leftarrow 0$ 
3:  $\log w_\eta \leftarrow \emptyset$ 
   // Define PLRV-O coefficients
4:  $b_1(\eta) \leftarrow \frac{\eta}{2\eta - 1}$ 
5:  $b_2(\eta) \leftarrow \frac{\eta - 1}{2\eta - 1}$ 
6:  $\alpha_1(\eta) \leftarrow C(\eta - 1)\theta$ 
7:  $\alpha_2(\eta) \leftarrow C\eta\theta$ 
8: for  $i = 1$  to  $N$  do
9:    $g \leftarrow \sqrt{i} - \sqrt{i - 1}$ 
10:   $\ell^F \leftarrow \emptyset$ 
11:  for  $\eta = 0$  to  $n$  do
   // Log binomial weights
12:     $\log w_\eta \leftarrow \log \binom{n}{\eta} + (n - \eta) \log(1 - \zeta) + \eta \log \zeta$ 
   // Log PLRV-O terms (for all  $\eta$ )
13:     $\ell^- \leftarrow \log b_1(\eta) - k \log(1 - \alpha_1(\eta)g)$ 
14:     $\ell^+ \leftarrow \log b_2(\eta) - k \log(1 + \alpha_2(\eta)g)$ 
15:     $\max_\ell \leftarrow \max(\ell^-, \ell^+)$ 
   // Two-branch merge (log-sum-exp)
16:     $\ell_\eta^F \leftarrow \max_\ell + \log(e^{\ell^- - \max_\ell} + e^{\ell^+ - \max_\ell})$ 
   // Combine with weights (log-sum-exp over  $\eta$ )
17:     $\ell_i \leftarrow \max_\eta \{\log w_\eta + \ell_\eta^F\} + \log \sum_\eta \exp(\log w_\eta + \ell_\eta^F - \max_\eta)$ 
18:     $\text{sum} \leftarrow \text{sum} + \ell_i$ 
19:  $\alpha_\lambda \leftarrow \text{sum}$ 
20: return  $\alpha_\lambda$ 

```

// can be parallelized

// logsum: can be parallelized

enough for convergence, further increases merely add distortion without improving accuracy.

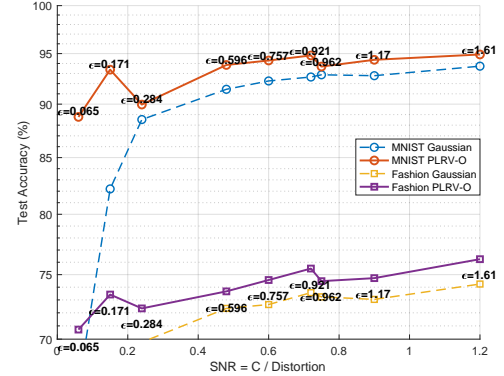


Figure 5: Signal-to-noise ratio (SNR) as a surrogate utility function for optimizing PLRV-O parameters.

For PLRV-O, however, clipping appears directly in the MAF equation. This coupling means the privacy-utility trade-off depends jointly on (k, θ, C) , with possible inflection points where changes in C alter the balance between distortion and privacy. Thus, unlike Gaussian, PLRV-O requires joint optimization over all three parameters rather than fixing the clip a priori. Figure 5 confirms that this SNR definition closely tracks accuracy across privacy budgets, with each point annotated by its ϵ value.

Motivated by this connection, we adopt an analogous SNR view for PLRV-O. In particular, we use the expected ℓ_1 -error (proved in Appendix C.3) as a tractable surrogate for distortion, and combine it with clipping to obtain

$$\text{SNR}(k, \theta, C) = \frac{C}{\ell_1(z)} = C(k - 1)\theta.$$

The distortion of PLRV-O noise, characterized in Theorem 5.1 (proved in Appendix C.3).

the effective noise multiplier σ/ζ captures learning degradation under a fixed budget, independent of C , since clipping cancels out in the SNR and does not appear in privacy accounting (only entering through the noise scale $\sigma(\epsilon) \times C$). Consequently, once C is large

THEOREM 5.1 (EXPECTED ℓ_1 -ERROR OF Γ -PLRV-O NOISE). Let z be PLRV-O noise with inverse scale u . Then the expected ℓ_1 -error is

$$\ell_1(z) = \mathbb{E}[\|z\|_1] = \int_0^\infty \mathcal{M}_u(-z) dz.$$

For $\Gamma(k, \theta)$ -PLRV-O noise with $k > 1$, this simplifies to $\ell_1(z) = \frac{1}{(k-1)\theta}$, and diverges otherwise.

This observation allows us to formulate PLRV-O parameter optimization directly as maximizing $J(k, \theta, C) = C(k-1)\theta$, subject to feasibility, stability, and privacy constraints.

The essential constraints arise from both distributional validity and the privacy budget:

c_0 -Clipping Bounds: $C_{\min} \leq C \leq C_{\max}$, where C_{\min} is the smallest value that ensures convergence and $C_{\max} \approx 2C_{\min}$ prevents unnecessary inflation.

Moment Generating Function: since $u \sim \Gamma(k, \theta)$ with $b = 1/u$, feasibility requires $\theta < 1/t$, equivalently $\lambda_{\max} C \theta < 1$, because

$$\mathcal{M}_u(t) = (1 - t\theta)^{-k}, \quad t < \frac{1}{\theta}.$$

With $C < 1$ in practice and typically $\theta < 10^{-3}$, this condition is loose, allowing $\lambda_{\max} \approx 10^3$.

c_1 -Laplace Scale-parameter Stability: $\text{GammaCDF}(0.1; k, \theta) \approx 0$, which suppresses configurations with $b > 10$ and avoids unstable noise regimes.

c_2 -Privacy Constraint: $\epsilon(\delta) \leftarrow \text{MAF_PLRV-O}(k, \theta, \zeta, T, C, \delta)$.

c_3 & c_4 -Distortion Constraints: $c_3 : k > 1$, $c_4 : \theta \geq \frac{0.1}{k-1}$.

Here c_3 ensures finite expected ℓ_1 -error, while c_4 caps distortion at 10, a threshold that in practice corresponds to unstable regimes with weak accuracy. Together, constraints c_0 - c_4 define the feasible search space, yielding the constrained optimization problem:

$$\max_{k, \theta, C} J(k, \theta, C) = C(k-1)\theta \quad \text{s.t.} \quad c_0 - c_4.$$

We solve this nonlinear program using a standard nonlinear constrained optimization routine, which accommodates bound, linear, and nonlinear constraints, to obtain the optimal (k^*, θ^*, C^*) .

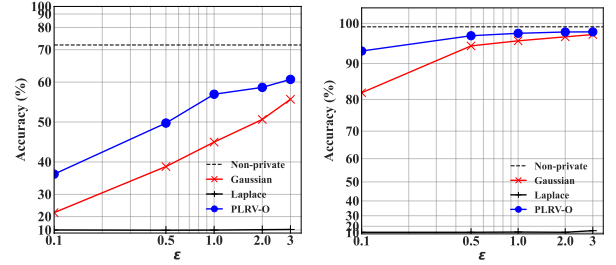
6 Evaluation

We evaluate DP-SGD with Gaussian and PLRV-O on computer vision (CV) and natural language processing (NLP) tasks, and aim to: (i) assess task utility, (ii) compare empirical privacy guarantees vs. theoretical counterparts, and (iii) analyze the role of the parameters k , θ , and C for interpretability of PLRV-O. Results on runtime, convergence, and boosting orthogonal methods are also provided.

6.1 Performance for CV Tasks

We evaluated our method with Gaussian-based DP-SGD on CIFAR-10, CIFAR-100 [37], and MNIST [38]. To demonstrate that the framework can optimize training noise from scratch, it was tested on three image classification models: a 4-layer CNN, a ResNet18, and a Vision Transformer (ViT) model with stride 16. The model sizes are about 26 thousand, 11 million, and 85 million, respectively. In these experiments, the clipping threshold has a wide range, from 0.3 to 15, and θ is very small (e.g., 5×10^{-4}), which is consistent with the theory that the parameter k controls the accuracy and θ controls the stability. The ideal result, then, will have *larger* k for

less destructive noise and thus better accuracy, while also having smaller θ for noise generation stability.



(a) ResNet18 with CIFAR-10 (b) Small CNN with MNIST

Figure 6: Model evaluation results for CV tasks.

Figure 6 presents the model utility across a range of privacy budgets ϵ , comparing Gaussian, Laplace, and PLRV-O mechanisms, on the convolutional network including ResNet18 and 4-layer CNN, trained on CIFAR-10 and CIFAR-100, respectively. Across both subplots, PLRV-O consistently outperforms Gaussian and Laplace. Specifically, for ResNet18 on CIFAR-10, PLRV-O achieves up to 30% higher accuracy than Gaussian under low privacy budgets. For ViT with CIFAR-10, PLRV-O surpasses Gaussian by approximately 10% (see Table 2). These results highlight the effectiveness of PLRV-O, especially in low privacy regimes, and demonstrate its robustness across both CNNs and transformer-based models.

Table 2: PLRV-O and Gaussian mechanisms for fine-tuning a ViT model (stride = 16). The base model was trained on ImageNet and fine-tuned on CIFAR-10. Noise parameters are (k, θ) for PLRV-O and σ for Gaussian.

	Acc. (%)	ϵ	Steps	S. rate	δ	Dist.	Clip	Noise Params
PLRV-O	93.63	1.7	250	0.01024	2×10^{-5}	8.58	10.0	$k=141.06$, $\theta=8.32 \times 10^{-4}$
PLRV-O	92.90	0.46	250	0.01024	2×10^{-5}	9.17	5.0	$k=5242.4$, $\theta=2.08 \times 10^{-5}$
Gaussian	89.01	1.7	250	0.01024	2×10^{-5}	3.77	5.0	$\sigma=0.9456$
Gaussian	83.93	0.46	250	0.01024	2×10^{-5}	22.51	15.0	$\sigma=1.8812$

Interpretability of PLRV-O Parameters. See Table 13–14 in Appendix E for results on multiple ϵ values in the high-privacy regime ($\epsilon \leq 1.6$) for the CNN model on the MNIST and Fashion-MNIST datasets. The optimized clipping threshold C , θ , and k for the given steps, q , δ were found. After training with these parameters, the PLRV-O performed far better than the Gaussian mechanism, with accuracy approaching training without noise. More results related to the optimized parameters are shown in Appendix D.1.

6.2 Performance for NLP Tasks

We also evaluate PLRV-O on two NLP tasks using language models: sentence classification and text generation.

6.2.1 Performance on Sentence Classification. Our evaluation is on GLUE benchmarks (SST-2: distinguish between positive and negative emotions; QNLI: determine whether a context sentence

contains the answer to a given question) [59] with experiments conducted on RoBERTa-base, RoBERTa-large [40], BERT-base, BERT-large [15], comparing performance with the non-private training and baseline DP-SGD method [39]. In detail, SST-2 has more than 60k+ samples in the training set, and QNLI has more than 100k+ samples; SST-2 and QNLI include two classes each. In this experiment, we use the full training and test sets.

In Figures 7 and 8, the x -axis shows total privacy loss ϵ , and the y -axis shows the accuracy under specific ϵ after T -step composition during fine-tuning. From (a) to (d) of Figures 7 and 8, the non-private model accuracy are 90.5, 92.7, 92.8, 94.7, 96.4, 94.9 94.8, and 96.4 respectively. When $\epsilon \leq 3$, our mechanism largely outperforms the baselines, exhibiting close performance with non-private training. Specifically, we can observe that the fine-tuning with the Laplace mechanism and ℓ_1 norm, the accuracy is around 50%, which means the model is not trainable since the language model is large and the ℓ_1 norm is much larger than the ℓ_2 norm of Gaussian noise. We can also observe that our performance (blue line) is better than the performance of the Gaussian mechanism with around 3% - 7%.

6.2.2 Performance on Text Generation Task. We experiment with the official pipeline on the E2E dataset [46] and DART dataset [45]. We fine-tune the DistilGPT2, GPT-2, GPT2-medium, and GPT2-large models on the E2E dataset with $\delta = 10^{-5}$, evaluating five metrics: BLEU, NIST, METEOR, ROUGE-L, and CIDEr. We evaluate PLRV-O and DP-SGD [39] under $\delta = 10^{-5}$. We also apply the same settings of privacy budget at each iteration, weights, and clipping threshold as in the sentence classification. We only employ a batch size of 1024, which causes the total privacy budget $\epsilon < 0.2$.

Table 3: DistilGPT2 model on the E2E dataset.

Noise	ϵ	BLEU	NIST	METEOR	ROUGE-L	CIDEr
Gaussian	0.2	25.29	0.3424	0.2304	0.4925	0.5883
	0.5	36.73	1.0098	0.2829	0.5733	0.7638
	1	50.55	3.5693	0.3225	0.6159	1.0901
	2.5	59.82	5.6407	0.3646	0.6589	1.5164
PLRV-O	0.2	58.50	5.3100	0.3578	0.6534	1.3862
	0.5	64.16	7.4953	0.3944	0.6681	1.8563
	1	63.63	7.2425	0.3894	0.6675	1.7844
	2.5	64.94	8.1061	0.4140	0.6790	2.0404

Table 4: GPT-2 model on the E2E dataset.

Noise	ϵ	BLEU	NIST	METEOR	ROUGE-L	CIDEr
Gaussian	0.2	32.82	0.6487	0.2733	0.5642	0.7618
	0.5	42.72	1.9037	0.3037	0.5887	0.9699
	1	52.11	3.7071	0.3313	0.6281	1.2369
	2.5	59.02	5.6853	0.3602	0.6520	1.5457
PLRV-O	0.2	60.21	5.7860	0.3688	0.6628	1.5285
	0.5	62.98	7.5666	0.4025	0.6767	1.9438
	1	62.73	7.0415	0.3928	0.6750	1.8164
	2.5	65.27	8.3764	0.4360	0.6858	2.2612

Tables 3-6 present the results with the five different metrics, following [63]. We observe that PLRV-O yields results that are more closely aligned with the non-private results than Gaussian (larger values of all these metrics exhibit more accurate generated texts). Note the improvement can be up to 50% on some metrics (e.g., CIDEr). Tables 7 and 8 show the generation performance for the DART dataset. We can observe a similar trend to the E2E dataset.

6.3 Moments Accountant

To validate the privacy accountant of our PLRV-O, we evaluate our privacy loss through T . In this experiment, we choose two different

Table 5: E2E evaluation results of GPT2-medium model under different noise types and privacy budgets (ϵ).

Noise	ϵ	BLEU	NIST	METEOR	ROUGE-L	CIDEr
Gaussian	0.2	37.38	1.4594	0.2870	0.5662	0.8094
	0.5	52.96	3.8638	0.3447	0.6206	1.2907
	1	59.00	6.0868	0.3709	0.6452	1.6023
	2.5	62.22	8.0526	0.4063	0.6684	1.9906
PLRV-O	0.2	58.79	6.1828	0.3792	0.6580	1.6706
	0.5	64.47	8.3884	0.4295	0.6789	2.2338
	1	63.67	8.3098	0.4220	0.6785	2.1590
	2.5	66.04	8.4342	0.4423	0.6922	2.3728

Table 6: E2E evaluation results of GPT2-large model under different noise types and privacy budgets (ϵ).

Noise	ϵ	BLEU	NIST	METEOR	ROUGE-L	CIDEr
Gaussian	0.2	39.25	1.9838	0.2940	0.5892	0.9242
	0.5	52.51	3.9813	0.3525	0.6421	1.1923
	1	53.59	4.6533	0.3317	0.6191	1.2980
	2.5	62.24	8.0916	0.4118	0.6661	2.0894
PLRV-O	0.2	60.71	6.4304	0.3743	0.6501	1.6485
	0.5	65.02	8.4223	0.4226	0.6740	2.0988
	1	64.21	8.3605	0.4179	0.6676	2.0811
	2.5	67.37	8.6457	0.4496	0.6952	2.3657

Table 7: DART evaluation results of DistilGPT2 model under different noise types and privacy budgets (ϵ).

Noise	ϵ	BLEU	NIST	METEOR	ROUGE-L	CIDEr
Gaussian	0.2	3.55	0.4290	0.0467	0.1023	0.2909
	0.5	12.47	2.1889	0.1300	0.2416	0.5654
	1	17.48	2.4004	0.1838	0.3291	0.8345
	2.5	22.26	3.9404	0.2156	0.3816	1.0045
PLRV-O	0.2	23.29	3.8109	0.2292	0.4040	1.1161
	0.5	28.42	4.0702	0.2701	0.4779	1.5073
	1	27.89	4.1538	0.2658	0.4688	1.4639
	2.5	30.83	4.5753	0.2841	0.5036	1.6856

Table 8: DART evaluation results of GPT-2 model under different noise types and privacy budgets (ϵ).

Noise	ϵ	BLEU	NIST	METEOR	ROUGE-L	CIDEr
Gaussian	0.2	6.95	0.0761	0.1293	0.2625	0.6065
	0.5	20.31	2.0213	0.2234	0.4222	1.0794
	1	25.31	3.3642	0.2549	0.4631	1.3252
	2.5	29.32	4.7652	0.2772	0.4900	1.5449
PLRV-O	0.2	25.95	2.5579	0.2699	0.4911	1.4419
	0.5	30.76	2.9106	0.2891	0.5123	1.6783
	1	31.38	3.2593	0.3029	0.5212	1.7453
	2.5	33.66	4.7260	0.3142	0.5407	1.9371

settings of C , θ , k , and ζ of our experiments with small distortion to show the privacy loss with T . For the Gaussian mechanism, we apply the same C and ζ to get the privacy loss with T with $\sigma = 0.1$. See Figure 9 for the results. For a large clip such as $C = 1.0$, the Gaussian mechanism and PLRV-O have similar privacy loss. However, the distortion of PLRV-O noise is lower, thus PLRV-O is the more desirable noise under the same privacy loss.

6.4 Privacy Audit

While we present theoretical privacy loss via T , we also report empirical ϵ under attacks. Using the auditing model in Appendix D.3, we conduct a privacy audit to validate our guarantees. Specifically, we implement a data poisoning attack with dataset and algorithm \mathcal{A} , generating a small poisoning set S of k points and a binary

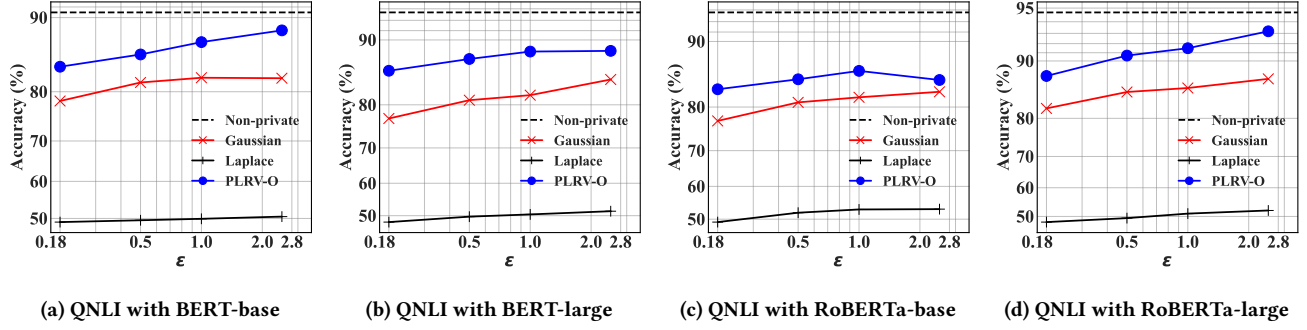


Figure 7: Model evaluation results for QNLI tasks using BERT and RoBERTa (Base and Large).

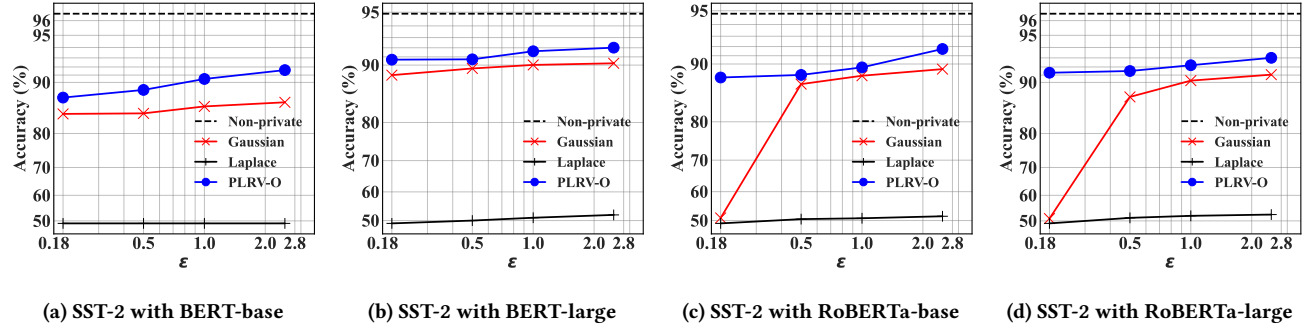


Figure 8: Model evaluation results for SST-2 tasks using BERT and RoBERTa (Base and Large).

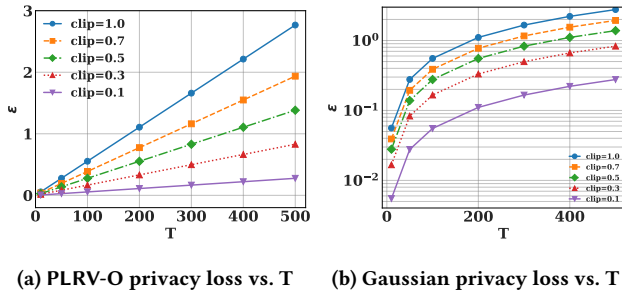


Figure 9: Privacy loss vs. T , clip. (a) $k = 414.2857$, $\theta = 2.4196 * 10^{-4}$, $q = 0.00977631$, $\delta = 10^{-5}$ and $N = 109482240$. (b) $\sigma = 0.1$.

classifier T that distinguishes $\mathcal{A}(D)$ from $\mathcal{A}(D \cup S)$ with significant advantage over random guessing.

We follow the auditing steps with ClipBKD, a clipping-aware backdoor attack robust to clipping [32]. For CV tasks, we use Fashion-MNIST [62] and Purchase-100 [53]; for NLP, SST-2 and QNLI. The ClipBKD test statistic checks if backdoored points are distinguishable by loss falling below a threshold. To set this threshold, we train models on unpoisoned and poisoned datasets differing by k samples. Poisoning points are generated with TextAttack and used to create neighborhood datasets D_0 and D_1 . Due to resource limits, we train 10 models ($T = 20$ trials) for threshold learning, then 20 models per dataset-model pair for testing on S to detect whether S was included. We set confidence at 0.01 (i.e., our Monte Carlo estimates hold with 99% confidence) to compute empirical ϵ_{LB} , reporting the best result for $k = 1$ poisoning point.

Figure 10 shows the provable ϵ (x-axis) and empirical ϵ (y-axis) for DP-SGD and PLRV-O for nlp task. It shows that the empirical privacy bound of DP-SGD and PLRV-O is less than the theoretical one. And our empirical privacy bound is less than DP-SGD, which means that our work can provide a stricter privacy guarantee than DP-SGD empirically, which also guarantees that the comparison of DP-SGD and PLRV-O is fair. Similar to the fine-tuning of NLP, we discuss the performance of the proposed work on the CV task in Figure 11. We evaluate the ClipBKD auditing experiments on the Logistic Regression (LR) model and the two-layer Feedforward Neural Network (FNN) with Fashion-MNIST and Purchase-100 datasets following the pipeline in [32]. The pattern we choose for backdoor attacks is a 5x5 white square in the top-left corner of an image, following [32]. To produce the threshold of backdoor attack, we train 500 models on the unpoisoned dataset and 500 models on the poisoned dataset, and produce the best ϵ_{LB} with other 1000 trained models using empirically measuring privacy in [32]. The empirical privacy of Gaussian and PLRV-O are similar, but they are still lower than the theoretical one. Thus, our work has strong potential for extensions to domains with training from scratch, such as CV and NLP tasks.

6.5 Runtime and Convergence Analysis

PLRV-O introduces negligible extra overhead. The primary cost is offline, involving a one-time search for the optimal (k, θ) pair and the precomputation of constants for noise sampling. PLRV-O often enables faster online runtime by supporting much larger clipping thresholds than Gaussian at the same ϵ , as shown in Table 9.

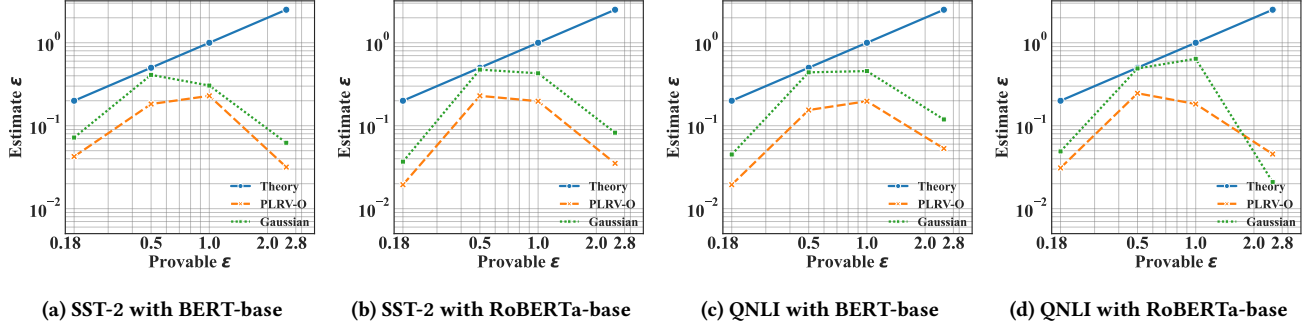


Figure 10: NLP performance of privacy attacks ClipBKD.

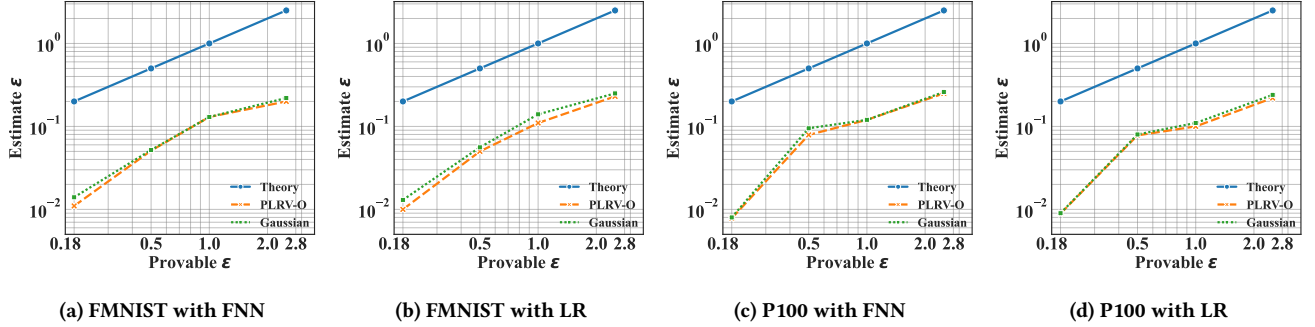


Figure 11: CV performance of privacy attacks ClipBKD.

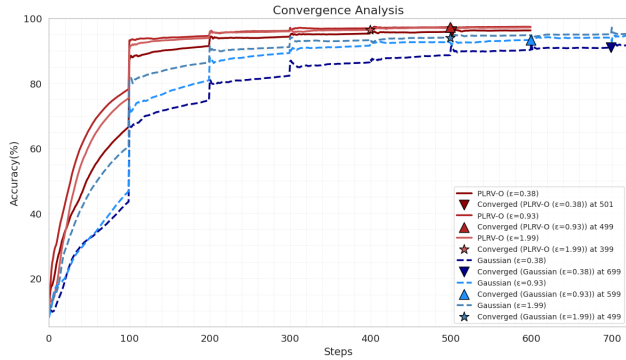


Figure 12: Training accuracy over training steps for PLRV-O and Gaussian mechanisms across different privacy budgets (ϵ). PLRV-O shows faster and more stable convergence compared to the Gaussian at equivalent privacy levels.

Convergence Analysis. We evaluate the effect of noise mechanisms on model convergence by comparing PLRV-O and Gaussian noise across different privacy budgets (ϵ). The convergence step is defined as the first point where the accuracy improvement within the previous 200 epochs falls below 1%. ΔAcc measures the change in accuracy from 200 steps before convergence to the convergence point. Table 9 summarizes the convergence step, accuracy at convergence, and ΔAcc (change in accuracy over the final 200 steps) during CNN training on the MNIST dataset.

As shown in Figure 12, PLRV-O achieves faster convergence and consistently higher accuracy compared to the Gaussian mechanism at equivalent ϵ values. This advantage stems from PLRV-O's ability

Table 9: Convergence comparison between Gaussian and PLRV-O mechanisms at different privacy levels (ϵ) during CNN training on the MNIST dataset.

Mechanism	ϵ	Con. Step	Acc. at Con.	ΔAcc	Time to Con. (s)
PLRV-O	0.38	501	95.55%	0.69%	57.60
	0.93	499	96.23%	0.14%	55.58
	1.99	399	96.44%	0.61%	44.73
Gaussian	0.38	699	91.00%	-0.19%	90.44
	0.93	599	93.31%	0.80%	61.16
	1.99	499	94.04%	-0.27%	51.35

to tolerate larger clipping bounds under the same privacy budget, accelerating training. Our empirical results show consistent convergence improvements. Furthermore, our PLRV-O mechanism can also be applied to large datasets to achieve a better privacy utility trade-off, such as ImageNet or TinyImageNet.

Table 10: Boosting DP-FTRL accuracy (%) on MNIST/CIFAR-10 ($\delta = 1/n$). The non-private accuracy is 98.9% for MNIST and 78.5% for CIFAR-10 (the latter from Figure 1b in [34]).

Dataset	ϵ	Gaussian Acc.	PLRV-O Acc.
MNIST	0.05	30.34%	92.07%
	0.23	95.15%	96.86%
	0.90	97.50%	98.28%
CIFAR-10	0.05	58.18%	68.55%
	0.23	76.09%	76.12%
	0.90	76.09%	76.12%

6.6 Boosting Orthogonal Methods

PLRV-O also provides an orthogonal improvement that can enhance the performance of existing methods. To demonstrate its applicability to advanced settings, we apply it to DP-FTRL [34] as a representative example. PLRV-O noise consistently outperforms Gaussian noise across different privacy budgets, demonstrating that PLRV-O can boost DP-FTRL in its applications (without subsampling) in Table 10, e.g., matrix factorization, federated learning [21].

7 Related Work

The majority of research on DP-SGD has focused on the Gaussian mechanism due to its smooth noise distribution, which aligns well with gradient updates and facilitates privacy accounting using the moments accountant framework [1].

Recent Development in DP-SGD. Several studies have been proposed for improving DP-SGD along different dimensions. They can be broadly categorized into: (i) memory-efficient methods: GHOST [39], PEFT [63], and ViP [64] reduce memory overhead by modifying gradient computation or clipping schemes; (ii) time-efficient methods: DP-SGD-JL [6], Mixed Ghost [7], and DP-BiTfIT [8] focus on reducing runtime while maintaining DP; and (iii) accuracy-enhancing methods: DPSUR [23], DP-Forward [16] improve utility by refining gradient updates or leveraging structured noise.

While most of them focus on the Gaussian mechanism, no existing DP-SGD variants have applied Laplace noise for large-scale NLP or vision tasks. Beyond efficiency improvements, prior work has also refined privacy analysis in DP-SGD. Wang et al. [61] examined subsampling effects on privacy guarantees, while Gopi et al. [27] developed a numerical approach to compute privacy loss precisely. These accounting refinements could be leveraged alongside PLRV-O to achieve tighter privacy budgets and faster convergence.

DP-SGD with Laplace Mechanism. Prior to the widespread adoption of DP-SGD, the Laplace mechanism was considered optimal in many DP applications due to its well-defined theoretical properties and robustness in certain regimes. It remains widely used in pure ϵ -DP settings, offering minimal ℓ_1 and ℓ_2 errors under strong privacy constraints [17, 25]. While Gaussian noise has become the standard in DP-SGD due to its compatibility with the moments accountant, Laplace noise can outperform Gaussian in certain privacy regimes, particularly as $\epsilon \rightarrow 0^+$, where it achieves lower error [25]. More recent works [54] have introduced privacy loss distribution (PLD)-based accounting, enabling tighter (ϵ, δ) -DP for Laplace, Gaussian, and Discrete Laplace mechanisms, especially under Poisson subsampling.

Despite these advantages, DP-SGD with Laplace noise has seen limited adoption due to the prohibitive nature of ℓ_1 -norm gradient clipping, which often destabilizes training and degrades privacy-utility trade-offs. Unlike Gaussian noise, which integrates well with ℓ_2 -norm clipping, Laplace noise interacts poorly with ℓ_1 -norm constraints, making its deployment in large-scale models challenging. Sommer et al. [54] analyzed Laplace DP-SGD through privacy loss random variables (PLRVs), comparing it with Gaussian mechanisms via a numerical approach leveraging the central limit theorem. In contrast, our work provides a structured privacy accounting framework that avoids such approximations.

A separate line of research, including Jang et al. [33] and Bernstein et al. [4], explores DP-signSGD, where gradients are compressed for efficient communication, with updates determined via majority voting rather than traditional DP-SGD averaging. Since DP-signSGD workers transmit only gradient signs, alternative privacy mechanisms such as the exponential and Laplace mechanisms have been studied in this context. However, as DP-signSGD follows a fundamentally different training paradigm, we consider it independent of our setting. Another application of Laplace noise is in Bayesian deep learning, as explored by Daxberger et al. [14], where Laplace approximations facilitate Bayesian inference, offering theoretical advantages and practical benefits in uncertainty estimation. This approach, however, is distinct from our work, as it focuses on Bayesian learning rather than private SGD training.

8 Conclusion

We introduced PLRV-O, a flexible framework for optimizing differentially private deep learning by leveraging the structure of the privacy loss random variable (PLRV). Unlike conventional mechanisms such as Gaussian or Laplace noise—which are constrained by a single tunable parameter—PLRV-O introduces a multi-parameter design space that better captures the complexity of real-world privacy-utility trade-offs. By explicitly incorporating factors such as model size, training duration, sampling strategy, and clipping thresholds, PLRV-O enables fine-grained control over noise shaping for both training and fine-tuning. Empirical results across CV and NLP tasks demonstrate substantial performance gains under strong privacy constraints, where the proposed method enhances model utility without compromising privacy guarantees. Beyond training and fine-tuning, we plan to explore optimizable randomization mechanisms and noise to support broader domains, including machine unlearning [44], certified robustness [30, 65], and attacks [31] via randomized smoothing.

Acknowledgments

We sincerely thank the anonymous reviewers for their constructive comments. This work is partially supported by the National Science Foundation (NSF) under Grants No. CNS-2302689, CNS-2308730, CNS-2319277, CNS-2432533, ITE-2452747, and ITE-2452749, as well as by a Cisco Research Award. Any opinions, findings, conclusions, or recommendations expressed in this paper are those of the authors and do not necessarily reflect the views of the funding agencies.

References

- [1] Martin Abadi, Andy Chu, Ian Goodfellow, H Brendan McMahan, Ilya Mironov, Kunal Talwar, and Li Zhang. 2016. Deep learning with differential privacy. In *CCS*. 308–318.
- [2] Borja Balle, Gilles Barthe, Marco Gaboardi, Justin Hsu, and Tetsuya Sato. 2020. Hypothesis Testing Interpretations and Rényi Differential Privacy. In *AISTATS*.
- [3] Borja Balle and Yu-Xiang Wang. 2018. Improving the Gaussian mechanism for differential privacy: Analytical calibration and optimal denoising. In *ICML*.
- [4] Jeremy Bernstein, Jiawei Zhao, Kamyar Azizzadenesheli, and Anima Anandkumar. 2019. signSGD with Majority Vote is Communication Efficient and Fault Tolerant. In *International Conference on Learning Representations (ICLR)*.
- [5] Paul T Boggs and Jon W Tolle. 1995. Sequential quadratic programming. *Acta numerica* 4 (1995), 1–51.
- [6] Zhiqi Bu, Sivakanth Gopi, Janardhan Kulkarni, Yin Tat Lee, Hanwen Shen, and Uthaporn Tantipongpipat. 2021. Fast and Memory Efficient Differentially Private-SGD via JL projections. *NeurIPS* 34 (2021), 19680–19691.
- [7] Zhiqi Bu, Jialin Mao, and Shiyun Xu. 2022. Scalable and efficient training of large convolutional neural networks with differential privacy. *NeurIPS* (2022).

- [8] Zhiqi Bu, Yu-Xiang Wang, Sheng Zha, and George Karypis. 2022. Differentially private bias-term only fine-tuning of foundation models. In *NeurIPS 2022 Workshop on Trustworthy and Socially Responsible Machine Learning (TSRML)*.
- [9] Mark Bun, Cynthia Dwork, Guy N. Rothblum, and Thomas Steinke. 2018. Composable and Versatile Privacy via Truncated CDP. In *STOC*. 74–86.
- [10] Richard H Byrd, Jean Charles Gilbert, and Jorge Nocedal. 2000. A trust region method based on interior point techniques for nonlinear programming. *Mathematical programming* 89, 1 (2000), 149–185.
- [11] Richard H Byrd, Mary E Hribar, and Jorge Nocedal. 1999. An interior point algorithm for large-scale nonlinear programming. *SIAM Journal on Optimization* 9, 4 (1999), 877–900.
- [12] Nicholas Carlini, Chang Liu, Úlfar Erlingsson, Jeremy Kos, and Dawn Song. 2019. The Secret Sharer: Evaluating and Testing Unintended Memorization in Neural Networks. In *USENIX Security*. 267–284.
- [13] Giovanni Cherubin, Boris Köpf, Andrew Paverd, Shruti Tople, Lukas Wutschitz, and Santiago Zanella-Béguelin. 2024. Closed-Form Bounds for DP-SGD against Record-level Inference Attacks. In *USENIX Security*. 4819–4836.
- [14] Erik Daxberger, Agustinus Kristiadi, Alexander Immer, Runa Eschenhagen, Matthias Bauer, and Philipp Hennig. 2021. Laplace redux-effortless bayesian deep learning. *NeurIPS* 34 (2021), 20089–20103.
- [15] Jacob Devlin, Ming-Wei Chang, Kenton Lee, and Kristina Toutanova. 2019. BERT: Pre-training of deep bidirectional transformers for language understanding. In *NAACL-HLT*. 4171–4186.
- [16] Minxin Du, Xiang Yue, Sherman SM Chow, Tianhao Wang, Chenyu Huang, and Huan Sun. 2023. Dp-forward: Fine-tuning and inference on language models with differential privacy in forward pass. In *CCS*. 2665–2679.
- [17] Cynthia Dwork. 2006. Differential Privacy. In *ICALP*. 1–12.
- [18] Cynthia Dwork, Krishnamurthy Kulkarni, Frank McSherry, Ilya Mironov, and Moni Naor. 2006. Our data, ourselves: Privacy via distributed noise generation. In *Advances in Cryptology—EUROCRYPT*. 486–503.
- [19] Cynthia Dwork, Aaron Roth, et al. 2014. The algorithmic foundations of differential privacy. *Foundations and Trends® in Theoretical Computer Science* (2014).
- [20] Cynthia Dwork, Guy N Rothblum, and Salil Vadhan. 2010. Boosting and differential privacy. In *FOCS*. 51–60.
- [21] Shuya Feng, Meisam Mohammady, Hanbin Hong, Shenao Yan, Ashish Kundu, Binghui Wang, and Yuan Hong. 2025. Harmonizing Differential Privacy Mechanisms for Federated Learning: Boosting Accuracy and Convergence. In *CODASPY*.
- [22] Shuya Feng, Meisam Mohammady, Han Wang, Xiaochen Li, Zhan Qin, and Yuan Hong. 2024. DPI: Ensuring Strict Differential Privacy for Infinite Data Streaming. In *IEEE Symposium on Security and Privacy*. 1009–1027.
- [23] Jie Fu, Qingqing Ye, Haibo Hu, Zhili Chen, Lulu Wang, Kuncan Wang, and Xun Ran. 2024. DPSUR: accelerating differentially private stochastic gradient descent using selective update and release. *Vldb* (2024).
- [24] Jonas Geiping, Hartmut Bauermeister, Hannah Dröge, and Michael Moeller. 2020. Inverting gradients - how easy is it to break privacy in federated learning?. In *NeurIPS*.
- [25] Quan Geng and Pramod Viswanath. 2014. The optimal mechanism in differential privacy. In *ISIT*. 2371–2375.
- [26] Quan Geng and Pramod Viswanath. 2015. The optimal noise-adding mechanism in differential privacy. *IEEE Transactions on Information Theory* (2015).
- [27] Sivakanth Gopi, Yin Tat Lee, and Lukas Wutschitz. 2021. Numerical composition of differential privacy. *NeurIPS* 34 (2021), 11631–11642.
- [28] Godfrey H Hardy. 1929. Some simple inequalities satisfied by convex functions. *Messenger Math.* 58 (1929), 145–152.
- [29] Naoise Holohan, Spiros Antonatos, Stefano Braghin, and Pól Mac Aonghusa. 2018. The bounded laplace mechanism in differential privacy. *arXiv preprint arXiv:1808.10410* (2018).
- [30] Hanbin Hong, Binghui Wang, and Yuan Hong. 2022. UniCR: Universally Approximated Certified Robustness via Randomized Smoothing. In *ECCV*.
- [31] Hanbin Hong, Xinyu Zhang, Binghui Wang, Zhongjie Ba, and Yuan Hong. 2024. Certifiable Black-Box Attacks with Randomized Adversarial Examples: Breaking Defenses with Provable Confidence. In *CCS*. 600–614.
- [32] Matthew Jagielski, Jonathan Ullman, and Alina Oprea. 2020. Auditing differentially private machine learning: How private is private SGD? *NeurIPS* (2020).
- [33] Jonggyu Jang, Seongjin Hwang, and Hyun Jong Yang. 2024. Rethinking DP-SGD in Discrete Domain: Exploring Logistic Distribution in the Realm of signSGD. In *ICML*.
- [34] Peter Kairouz, Brendan McMahan, Shuang Song, Om Thakkar, Abhradeep Thakurta, and Zheng Xu. 2021. Practical and private (deep) learning without sampling or shuffling. In *ICML*. 5213–5225.
- [35] Peter Kairouz, Sewoong Oh, and Pramod Viswanath. 2015. The composition theorem for differential privacy. In *ICML*. 1376–1385.
- [36] Peter Kairouz, Sewoong Oh, and Pramod Viswanath. 2017. The Composition Theorem for Differential Privacy. *IEEE Information Theory* (2017), 4037–4049.
- [37] Alex Krizhevsky, Geoffrey Hinton, et al. 2009. Learning multiple layers of features from tiny images. (2009).
- [38] Yann LeCun, Léon Bottou, Yoshua Bengio, and Patrick Haffner. 1998. Gradient-based learning applied to document recognition. *Proc. IEEE* 86, 11 (1998).
- [39] Xuechen Li, Florian Tramer, Percy Liang, and Tatsunori Hashimoto. 2022. Large Language Models Can Be Strong Differentially Private Learners. In *ICLR*.
- [40] Yinhan Liu, Myle Ott, Naman Goyal, Jingfei Du, Mandar Joshi, Danqi Chen, Omer Levy, Mike Lewis, Luke Zettlemoyer, and Veselin Stoyanov. 2020. RoBERTa: A Robustly Optimized BERT Pretraining Approach. In *ICLR*.
- [41] Albert W Marshall, Ingram Olkin, and Barry C Arnold. 1979. Inequalities: theory of majorization and its applications. (1979).
- [42] Ilya Mironov, Kunal Talwar, and Li Zhang. 2019. Rényi Differential Privacy of the Sampled Gaussian Mechanism. In *NeurIPS*.
- [43] Meisam Mohammady, Shangyu Xie, Yuan Hong, Mengyuan Zhang, Lingyu Wang, Makan Pourzandi, and Mourad Debbabi. 2020. R2dp: A universal and automated approach to optimizing the randomization mechanisms of differential privacy for utility metrics with no known optimal distributions. In *CCS*.
- [44] Nima Naderlou, Shenao Yan, Binghui Wang, Jie Fu, Wendy Hui Wang, Weiran Liu, and Yuan Hong. 2025. Rectifying Privacy and Efficacy Measurements in Machine Unlearning: A New Inference Attack Perspective. In *USENIX Security*.
- [45] Linyong Nan, Dragomir Radev, Rui Zhang, Amrit Rau, Abhinand Sivaprasad, Chiachun Hsieh, Xiangru Tang, Aadit Vyas, Neha Verma, Pranav Krishna, Yangxiaokang Liu, Nadia Irwanto, Jessica Pan, Faiaz Rahman, Ahmad Zaidi, Mutethia Mutuma, Yasin Tarabar, Ankit Gupta, Tao Yu, Yi Chern Tan, Xi Victoria Lin, Caiming Xiong, Richard Socher, and Nazneen Fatema Rajani. 2021. DART: Open-Domain Structured Data Record to Text Generation. In *ACL-HLT*. 432–447.
- [46] Ekaterina Novikova, Ondřej Dušek, and Verena Rieser. 2017. The E2E Dataset: New Challenges For End-to-End Generation. (2017).
- [47] Constrained Nonlinear Optimization. 2025. <https://www.mathworks.com/help/optim/ug/constrained-nonlinear-optimization-algorithms.html>. (2025).
- [48] Josip E Peajcariac and Yung Liang Tong. 1992. *Convex functions, partial orderings, and statistical applications*. Academic Press.
- [49] Gege Qi, Yuefeng Chen, Xiaofeng Mao, Binyuan Hui, Xiaodan Li, Rong Zhang, and Hui Xue. 2023. Model Inversion Attack via Dynamic Memory Learning. In *MM*. 5614–5622.
- [50] Ahmed Salem, Apratim Bhattacharya, Michael Backes, Mario Fritz, and Yang Zhang. 2020. Updates-Leak: Data Set Inference and Reconstruction Attacks in Online Learning. In *USENIX Security* 20. 1291–1308.
- [51] Tom Sander, Pierre Stock, and Alexandre Sablayrolles. 2023. TAN without a burn: scaling laws of DP-SGD. In *ICML*.
- [52] Issai Schur. 1923. Über eine Klasse von Mittelbildungen mit Anwendungen auf die Determinantentheorie. *Sitzungsberichte der Berliner Mathematischen Gesellschaft* 22, 9–20 (1923), 51.
- [53] Reza Shokri, Marco Stronati, Congzheng Song, and Vitaly Shmatikov. 2017. Membership inference attacks against machine learning models. In *2017 IEEE Symposium on Security and Privacy (SP)*. IEEE, 3–18.
- [54] David Sommer, Sebastian Meiser, and Esfandiari Mohammadi. 2018. Privacy loss classes: The central limit theorem in differential privacy. *Cryptology ePrint Archive* (2018).
- [55] J. Michael Steele. 2004. *The Cauchy-Schwarz Master Class: An Introduction to the Art of Mathematical Inequalities*. Cambridge University Press.
- [56] Michel Talagrand. 1996. Majorizing Measures: The Generic Chaining. *The Annals of Probability* 24, 3 (1996), 1049–1103.
- [57] Sasha Targ, Diogo Almeida, and Kevin Lyman. 2016. Resnet in Resnet: Generalizing Residual Architectures. In *ICLR Workshop*.
- [58] Adrian M. Walker. 1965. Probability Theory and Mathematical Statistics. *The Mathematical Gazette* 49 (1965), 109 – 112.
- [59] Alex Wang, Amanpreet Singh, Julian Michael, Felix Hill, Omer Levy, and Samuel R. Bowman. 2019. GLUE: A Multi-Task Benchmark and Analysis Platform for Natural Language Understanding. In *ICLR*.
- [60] Chendi Wang, Yuqing Zhu, Weijie J Su, and Yu-Xiang Wang. 2024. Neural Collapse meets Differential Privacy: Curious behaviors of NoisyGD with Near-Perfect Representation Learning. In *ICML*, Vol. 235. 52334–52360.
- [61] Yu-Xiang Wang, Borja Balle, and Shiva Prasad Kasiviswanathan. 2019. Subsampled rényi differential privacy and analytical moments accountant. In *AISTATS*.
- [62] Han Xiao, Kashif Rasul, and Roland Vollgraf. 2017. Fashion-MNIST: a Novel Image Dataset for Benchmarking Machine Learning Algorithms. *arXiv preprint arXiv:1708.07747* (2017).
- [63] Da Yu, Saurabh Naik, et al. 2021. Differentially Private Fine-tuning of Language Models. In *ICLR*.
- [64] Yaodong Yu, Maziar Sanjabi, Yi Ma, Kamalika Chaudhuri, and Chuan Guo. 2023. Vip: A differentially private foundation model for computer vision. *arXiv preprint arXiv:2306.08842* (2023).
- [65] Xinyu Zhang, Hanbin Hong, Yuan Hong, Peng Huang, Binghui Wang, Zhongjie Ba, and Kui Ren. 2024. Text-CRS: A Generalized Certified Robustness Framework against Textual Adversarial Attacks. In *IEEE Symposium on Security and Privacy*.
- [66] Ligeng Zhu, Zhijian Liu, and Song Han. 2019. *Deep leakage from gradients*. Curran Associates Inc., Red Hook, NY, USA.

A Probability Theory Backgrounds

A.1 Moment Generating Function (MGF)

Definition A.1. Let $f(x)$ be the probability density function (PDF) of a random variable X . The moment generating function of X , if it exists, is defined as:

$$\mathcal{M}_X(t) = \mathbb{E}[e^{tX}] = \int e^{tx} f(x) dx.$$

THEOREM A.2 (COMPOSABILITY OF MGF). *If x_1, \dots, x_n are n independent random variables with existing MGFs $\mathcal{M}_{x_i}(t) = \mathbb{E}[e^{tx_i}]$ for $i = 1, \dots, n$, then the MGF of the linear combination $Y = \sum_{i=1}^n a_i x_i$ is given by:*

$$\mathcal{M}_Y(t) = \prod_{i=1}^n \mathcal{M}_{x_i}(a_i t).$$

B Laplace Mechanism Proofs

B.1 Proof of Theorem 4.1

In the following, we prove the bound on the privacy loss of the Laplace mechanism stated in Theorem 4.1.

Proof: Let $\tilde{g}(\text{aux}, \mathbf{x}, b)$ denote the output of a Laplace mechanism with scale b . The privacy loss at an outcome o is defined as:

$$c(o; \text{aux}, d, d', b) = \log \frac{\Pr[\tilde{g}(\text{aux}, \mathbf{x}, b) = o]}{\Pr[\tilde{g}(\text{aux}, -, b) = o]}, \quad (21)$$

where $\tilde{g}(\text{aux}, -, b)$ denotes the outcome of the mechanism without access to the input \mathbf{x} (e.g., \mathbf{x} is only in one data set). Thus, without loss of generality, the denominator follows a zero-mean Laplace PDF, as in the worst-case setting it lacks any gradient component in the direction of \tilde{g} , while the numerator is centered around \tilde{g} .

$$\begin{aligned} c(o; \text{aux}, d, d', b) &= \log \frac{\text{Lap}(\tilde{g}(\mathbf{x}), bI_n)}{\text{Lap}(0, bI_n)} \\ &= \log \frac{\left(\frac{1}{2b}\right)^n \exp\left(-\frac{\|o - \tilde{g}(\mathbf{x})\|_1}{b}\right)}{\left(\frac{1}{2b}\right)^n \exp\left(-\frac{\|o\|_1}{b}\right)} = \frac{\|o\|_1 - \|o - \tilde{g}(\mathbf{x})\|_1}{b}. \end{aligned}$$

For all real valued vectors A and B , using $\|A\|_1 = \|(A - B) + B\|_1$, by the triangle inequality we have: $\|A\|_1 - \|B\|_1 \leq \|A - B\|_1$. Thus,

$$\frac{\|o\|_1 - \|o - \tilde{g}(\mathbf{x})\|_1}{b} \leq \frac{\|\tilde{g}(\mathbf{x})\|_1}{b} \quad (22)$$

Evaluating the ℓ_1 norm in terms of the elements of $\tilde{g}(\mathbf{x}) = [g_1, g_2, \dots, g_n]$, we have:

$$c(o; \text{aux}, d, d', b) \leq \frac{\sum_{j=1}^n |g_j|}{b}. \quad (23)$$

B.2 Proof of Theorem 4.2

In the following, we prove a tight bound on the moments accountant function of univariate Laplace mechanisms, as stated in Theorem 4.2.

Proof: Consider two adjacent data sets d and d' . Without loss of generality, suppose d' has an extra training sample. Let ζ denote a fixed sampling rate. Consider any sampling realization over $d \cup d' = d'$ using iid sampling with per-element selection of ζ .

With probability $1 - \zeta$, the extra sample in d' will not be included and thus query values over the sub-sampled datasets will be identical. Let μ_0 denote the resulting density of the Laplace mechanism

in this case. Let $q(d, \zeta)$ denote the mean of μ_0 . By construction $|q(d, \zeta)| \leq C$.

With probability ζ , the extra sample in d' will be kept resulting in different query values between the two data sets. Let μ_1 denote the resulting density of the Laplace mechanism of the query over the sub-sampled d' . Let $q(d', \zeta)$ denote the mean of μ_1 . By construction $|q(d', \zeta)| \leq C$.

Thus, we can identify the mechanism over d' as having a mixture distribution,

$$M_q(d, \zeta) \sim \mu_0, \quad M_q(d', \zeta) \sim \mu \triangleq (1 - \zeta)\mu_0 + \zeta\mu_1.$$

For any λ , we aim to show:

$$A = \mathbb{E}_{z \sim \mu} \left[\left(\frac{\mu(z)}{\mu_0(z)} \right)^\lambda \right] \leq \alpha, \text{ and } B = \mathbb{E}_{z \sim \mu_0} \left[\left(\frac{\mu_0(z)}{\mu(z)} \right)^\lambda \right] \leq \alpha.$$

for some explicit α to be determined later.

Multiplying by $\mu_0(z)/\mu_0(z)$ and rearranging, we can express:

$$A = \mathbb{E}_{z \sim \mu_0} \left[\left(\frac{\mu(z)}{\mu_0(z)} \right)^{\lambda+1} \right] = \mathbb{E}_{z \sim \mu_0} \left[\left(1 - \zeta + \zeta \frac{\mu_1(z)}{\mu_0(z)} \right)^{\lambda+1} \right],$$

and

$$\begin{aligned} B &= \mathbb{E}_{z \sim \mu_0} \left[\left(\frac{\mu_0(z)}{(1 - \zeta)\mu_0(z) + \zeta\mu_1(z)} \right)^\lambda \right] \\ &= \mathbb{E}_{z \sim \mu_0} \left[\left(\frac{1}{1 - \zeta + \zeta \frac{\mu_1(z)}{\mu_0(z)}} \right)^\lambda \right]. \end{aligned} \quad (24)$$

Mironov et al. [42] (Section 3.1) demonstrate that $A \geq B$ holds in general for centrally symmetric distributions.

We thus focus on analyzing A . We start by applying the binomial theorem and the linearity of expectation,

$$\begin{aligned} A &= \mathbb{E}_{z \sim \mu_0} \left[\left(1 - \zeta + \zeta \frac{\mu_1(z)}{\mu_0(z)} \right)^{\lambda+1} \right] \\ &= \mathbb{E}_{z \sim \mu_0} \left[\sum_{\eta=0}^{\lambda+1} \binom{\lambda+1}{\eta} (1 - \zeta)^{\lambda+1-\eta} \zeta^\eta \left(\frac{\mu_1(z)}{\mu_0(z)} \right)^\eta \right] \\ &= \sum_{\eta=0}^{\lambda+1} \binom{\lambda+1}{\eta} (1 - \zeta)^{\lambda+1-\eta} \zeta^\eta \mathbb{E}_{z \sim \mu_0} \left[\left(\frac{\mu_1(z)}{\mu_0(z)} \right)^\eta \right]. \end{aligned}$$

We can simplify the ratio of the densities as

$$\begin{aligned} \frac{\mu_1(z)}{\mu_0(z)} &= \frac{\frac{1}{2b} \exp\left(-\frac{|z - q(d', \zeta)|}{b}\right)}{\frac{1}{2b} \exp\left(-\frac{|z - q(d, \zeta)|}{b}\right)} \\ &= \exp\left(\frac{1}{b} (|z - q(d, \zeta)| - |z - q(d', \zeta)|)\right). \end{aligned}$$

Without loss of generality, consider that $q(d, \zeta) < q(d', \zeta)$. We split up the real line into three intervals: $\mathbb{R} = (-\infty, q(d, \zeta)] \cup (q(d, \zeta), q(d', \zeta)) \cup [q(d', \zeta), \infty)$.

We evaluate the expectation $\mathbb{E}_{z \sim \mu_0} \left[\left(\frac{\mu_1(z)}{\mu_0(z)} \right)^\eta \right]$ over these three intervals separately (conditionally) and then will combine them afterwards (with probabilities of respective events occurring). We will analyze the middle interval last.

Case A1: $z < q(d, \zeta)$:

Since $z < q(d, \zeta)$, $|z - q(d, \zeta)| = q(d, \zeta) - z$. Likewise, $z < q(d', \zeta)$, so $|z - q(d', \zeta)| = q(d', \zeta) - z$. The likelihood ratio simplifies

$$\begin{aligned}\frac{\mu_1(z)}{\mu_0(z)} &= \exp\left(\frac{1}{b} (|z - q(d, \zeta)| - |z - q(d', \zeta)|)\right) \\ &= \exp\left(\frac{1}{b} (q(d, \zeta) - z - (q(d', \zeta) - z))\right) \\ &= \exp\left(\frac{1}{b} (q(d, \zeta) - q(d', \zeta))\right).\end{aligned}$$

We observe that there is no dependence on z , so this ratio becomes a constant in the expectation. Under μ_0 , z is equally distributed about $q(d, \zeta)$. So the probability of this event is $1/2$. Thus, the contribution to the total expectation is

$$\frac{1}{2} \exp\left(\frac{\eta}{b} (q(d, \zeta) - q(d', \zeta))\right).$$

Case A2: $z > q(d', \zeta)$: Since $z > q(d', \zeta)$, $|z - q(d', \zeta)| = z - q(d', \zeta)$. Likewise, $z > q(d, \zeta)$, so $|z - q(d, \zeta)| = z - q(d, \zeta)$. The likelihood ratio simplifies

$$\begin{aligned}\frac{\mu_1(z)}{\mu_0(z)} &= \exp\left(\frac{1}{b} (|z - q(d, \zeta)| - |z - q(d', \zeta)|)\right) \\ &= \exp\left(\frac{1}{b} (z - q(d, \zeta) - (z - q(d', \zeta)))\right) \\ &= \exp\left(\frac{1}{b} (q(d', \zeta) - q(d, \zeta))\right).\end{aligned}$$

Again, the ratio is a constant with respect to z . The probability of the event is more complicated to analyze than the previous event.

$$\begin{aligned}&\int_{q(d', \zeta)}^{\infty} \frac{1}{2b} \exp\left(-\frac{|z - q(d, \zeta)|}{b}\right) db \\ &= \int_{q(d', \zeta)}^{\infty} \frac{1}{2b} \exp\left(-\frac{z - q(d, \zeta)}{b}\right) db \\ &= \frac{1}{2b} \exp\left(\frac{q(d, \zeta)}{b}\right) \int_{q(d', \zeta)}^{\infty} \exp\left(-\frac{z}{b}\right) db \\ &= \frac{1}{2b} \exp\left(\frac{q(d, \zeta)}{b}\right) \frac{1}{-\frac{1}{b}} \exp\left(-\frac{z}{b}\right) \Big|_{q(d', \zeta)}^{\infty} \\ &= \frac{1}{2} \exp\left(\frac{q(d, \zeta)}{b}\right) \exp\left(-\frac{q(d', \zeta)}{b}\right) \\ &= \frac{1}{2} \exp\left(\frac{q(d, \zeta) - q(d', \zeta)}{b}\right)\end{aligned}$$

Thus, the contribution to the total expectation is

$$\begin{aligned}&\frac{1}{2} \exp\left(\frac{q(d, \zeta) - q(d', \zeta)}{b}\right) \exp\left(\frac{\eta}{b} (q(d', \zeta) - q(d, \zeta))\right) \\ &= \frac{1}{2} \exp\left(\frac{\eta - 1}{b} (q(d', \zeta) - q(d, \zeta))\right).\end{aligned}$$

Case A3: $q(d, \zeta) \leq z \leq q(d', \zeta)$:

Since $z > q(d, \zeta)$, $|z - q(d, \zeta)| = z - q(d, \zeta)$. Since $z < q(d', \zeta)$, so $|z - q(d', \zeta)| = q(d', \zeta) - z$. The likelihood ratio simplifies

$$\begin{aligned}\frac{\mu_1(z)}{\mu_0(z)} &= \exp\left(\frac{1}{b} (|z - q(d, \zeta)| - |z - q(d', \zeta)|)\right) \\ &= \exp\left(\frac{1}{b} (z - q(d, \zeta) - (q(d', \zeta) - z))\right) \\ &= \exp\left(\frac{1}{b} (-q(d, \zeta) - q(d', \zeta) + 2z)\right).\end{aligned}$$

Plugging this back into the expectation,

$$\begin{aligned}\mathbb{E}_{z \sim \mu_0} \left[\left(\frac{\mu_1(z)}{\mu_0(z)} \right)^\eta \right] &= \mathbb{E}_{z \sim \mu_0} \left[\exp\left(\frac{\eta}{b} (-q(d, \zeta) - q(d', \zeta) + 2z)\right) \right] \\ &= \exp\left(\frac{\eta}{b} (-q(d, \zeta) - q(d', \zeta))\right) \\ &\quad \times \mathbb{E}_{z \sim \mu_0} \left[\exp\left(\frac{2\eta z}{b}\right) \right].\end{aligned}$$

Evaluating the inner expectation (only over the interval here),

$$\begin{aligned}\mathbb{E}_{z \sim \mu_0} \left[\exp\left(\frac{2\eta z}{b}\right) \right] &= \int_{q(d, \zeta)}^{q(d', \zeta)} \frac{1}{2b} \exp\left(-\frac{|z - q(d, \zeta)|}{b} + \frac{2\eta z}{b}\right) db \\ &= \frac{1}{2b} \exp\left(\frac{q(d, \zeta)}{b}\right) \int_{q(d, \zeta)}^{q(d', \zeta)} \exp\left(z\left(-\frac{1 - 2\eta}{b}\right)\right) db \\ &= \frac{1}{2b} \exp\left(\frac{q(d, \zeta)}{b}\right) \frac{b}{2\eta - 1} \left[\exp\left(q(d', \zeta)\left(-\frac{1 - 2\eta}{b}\right)\right) \right. \\ &\quad \left. - \exp\left(q(d, \zeta)\left(-\frac{1 - 2\eta}{b}\right)\right) \right] \\ &= \frac{1}{2(2\eta - 1)} \left[\exp\left(q(d', \zeta) \frac{2\eta - 1}{b} + q(d, \zeta) \frac{1}{b}\right) \right. \\ &\quad \left. - \exp\left(q(d, \zeta) \frac{2\eta}{b}\right) \right].\end{aligned}$$

Thus, the contribution to the expectation from this case is

$$\begin{aligned}\mathbb{E}_{z \sim \mu_0} \left[\left(\frac{\mu_1(z)}{\mu_0(z)} \right)^\eta \right] &= \exp\left(\frac{\eta}{b} (-q(d, \zeta) - q(d', \zeta))\right) \\ &\quad \times \frac{1}{2(2\eta - 1)} \left[\exp\left(q(d', \zeta) \frac{2\eta - 1}{b} + q(d, \zeta) \frac{1}{b}\right) \right. \\ &\quad \left. - \exp\left(q(d, \zeta) \frac{2\eta}{b}\right) \right].\end{aligned}$$

Combining Cases A1-A3: Combining the results, we have that

$$\begin{aligned}A &= \mathbb{E}_{z \sim \mu_0} \left[\left(\frac{\mu(z)}{\mu_0(z)} \right)^{\lambda+1} \right] \\ &= \frac{1}{2} \exp\left(\frac{\eta}{b} (q(d, \zeta) - q(d', \zeta))\right) \\ &\quad + \frac{1}{2} \exp\left(\frac{\eta - 1}{b} (q(d', \zeta) - q(d, \zeta))\right) \\ &\quad + \exp\left(\frac{\eta}{b} (-q(d, \zeta) - q(d', \zeta))\right) \\ &\quad \times \frac{1}{2(2\eta - 1)} \left[\exp\left(q(d', \zeta) \frac{2\eta - 1}{b} + q(d, \zeta) \frac{1}{b}\right) \right. \\ &\quad \left. - \exp\left(q(d, \zeta) \frac{2\eta}{b}\right) \right]\end{aligned}$$

Recall that the query values over the sub-sampled data sets $q(d, \zeta)$ and $q(d', \zeta)$ are averaged over the queries (gradients) of the included samples, so the effect of a single sample is smaller the more samples are included. For simplicity, by inspection of the formula, we consider a worst case bound using $q(d) = 0$ and $q(d', \zeta) = C$.

$$\begin{aligned}
A &= \frac{1}{2} \exp\left(\frac{-\eta C}{b}\right) \\
&\quad + \frac{1}{2} \exp\left(\frac{(\eta-1)C}{b}\right) \\
&\quad + \exp\left(\frac{-\eta C}{b}\right) \frac{1}{2(2\eta-1)} \left[\exp\left(\frac{(\eta-1)C}{b}\right) - \exp(0) \right] \\
&= \exp\left(\frac{-\eta C}{b}\right) \left[\frac{1}{2} - \frac{1}{2(2\eta-1)} \right] \\
&\quad + \exp\left(\frac{(\eta-1)C}{b}\right) \left[\frac{1}{2} + \frac{1}{2(2\eta-1)} \right] \\
&= \exp\left(\frac{-\eta C}{b}\right) \left[\frac{\eta-1}{2\eta-1} \right] + \exp\left(\frac{(\eta-1)C}{b}\right) \left[\frac{\eta}{2\eta-1} \right]. \quad (25)
\end{aligned}$$

Analysis for B: Following the argument in Proof B.2 (Theorem 3.2), and using binomial expansion with term-wise comparison, we find that $B \geq A$, consistent with the result of Mironov et al.

B.3 Proof of Theorem 4.3

In the following, we prove Theorem 4.3, that the moments accounting function of the univariate Laplace mechanism is Schur-convex. We first prove the following technical lemma, involving second derivatives of the MAF, before continuing on to the main proof.

LEMMA B.1. *The second derivative of the moments accountant function $\alpha(\lambda)$ in Theorem 4.2 with respect to the marginal clipped gradients $|g_i|$ is non-negative.*

Proof: Let $a_\eta = \binom{\lambda+1}{\eta} (1-\zeta)^{\lambda+1-\eta} \zeta^\eta$ be the positive weight associated with each η . The second derivative of $\alpha(\lambda)$ can be written as

$$\frac{d^2 \alpha(\lambda)}{d|g_i|^2} = \frac{\left(\sum_\eta a_\eta F(|g_i|, \eta) \right) \left(\sum_\eta a_\eta \frac{d^2 F}{d|g_i|^2} \right) - \left(\sum_\eta a_\eta \frac{dF}{d|g_i|} \right)^2}{\left(\sum_\eta a_\eta F(|g_i|, \eta) \right)^2}.$$

Recall:

$$\begin{aligned}
F(|g_i|, \eta) &= \frac{\eta}{2\eta-1} e^{\frac{(\eta-1)|g_i|}{b}} + \frac{\eta-1}{2\eta-1} e^{-\frac{\eta|g_i|}{b}}, \\
\frac{dF}{d|g_i|} &= \frac{\eta(\eta-1)}{b(2\eta-1)} \left(e^{\frac{(\eta-1)|g_i|}{b}} - e^{-\frac{\eta|g_i|}{b}} \right), \\
\frac{d^2 F}{d|g_i|^2} &= \frac{\eta(\eta-1)}{b^2(2\eta-1)} \left((\eta-1) e^{\frac{(\eta-1)|g_i|}{b}} + \eta e^{-\frac{\eta|g_i|}{b}} \right).
\end{aligned}$$

Expand $F \times F''$:

$$\begin{aligned}
F \times F'' &= \left(\frac{\eta}{2\eta-1} e^{\frac{(\eta-1)|g_i|}{b}} + \frac{\eta-1}{2\eta-1} e^{-\frac{\eta|g_i|}{b}} \right) \\
&\quad \times \frac{\eta(\eta-1)}{b^2(2\eta-1)} \left((\eta-1) e^{\frac{(\eta-1)|g_i|}{b}} + \eta e^{-\frac{\eta|g_i|}{b}} \right) \\
&= \frac{\eta(\eta-1)}{b^2(2\eta-1)^2} \left[\eta(\eta-1) e^{2\frac{(\eta-1)|g_i|}{b}} + \eta^2 e^{\frac{(\eta-1)|g_i|/b}{-}} \eta |g_i|/b \right. \\
&\quad \left. + (\eta-1)^2 e^{-\frac{\eta|g_i|}{b} + \frac{(\eta-1)|g_i|}{b}} + \eta(\eta-1) e^{-2\frac{\eta|g_i|}{b}} \right].
\end{aligned}$$

Notice:

$$e^{\frac{(\eta-1)|g_i|}{b}} e^{-\frac{\eta|g_i|}{b}} = e^{-\frac{|g_i|}{b}}, \quad e^{-\frac{\eta|g_i|}{b}} e^{\frac{(\eta-1)|g_i|}{b}} = e^{-\frac{|g_i|}{b}}.$$

Thus:

$$\begin{aligned}
F \times F'' &= \frac{\eta(\eta-1)}{b^2(2\eta-1)^2} \times \\
&\quad \left[\eta(\eta-1) e^{2\frac{(\eta-1)|g_i|}{b}} + (\eta^2 + (\eta-1)^2) e^{-\frac{|g_i|}{b}} + \eta(\eta-1) e^{-2\frac{\eta|g_i|}{b}} \right].
\end{aligned}$$

Expand $\left(\frac{dF}{d|g_i|} \right)^2$:

$$\begin{aligned}
\left(\frac{dF}{d|g_i|} \right)^2 &= \left(\frac{\eta(\eta-1)}{b(2\eta-1)} \right)^2 \left(e^{\frac{(\eta-1)|g_i|}{b}} - e^{-\frac{\eta|g_i|}{b}} \right)^2 \\
&= \left(\frac{\eta(\eta-1)}{b(2\eta-1)} \right)^2 \left(e^{2\frac{(\eta-1)|g_i|}{b}} - 2e^{-\frac{|g_i|}{b}} + e^{-2\frac{\eta|g_i|}{b}} \right).
\end{aligned}$$

Comparing individual terms pointwise shows that $F \times F'' \geq (F')^2$ holds for all $|g_i| \geq 0$ and $\eta \geq 0$. Applying the Cauchy-Schwarz inequality to the positive sequence $\{\sqrt{a_\eta} \sqrt{F(|g_i|, \eta)}\}$ and $\{\sqrt{a_\eta} \sqrt{d^2 F/d|g_i|^2}\}$ yields

$$\left(\sum_\eta a_\eta \sqrt{F(|g_i|, \eta)} \sqrt{\frac{d^2 F}{d|g_i|^2}} \right)^2 \leq \left(\sum_\eta a_\eta F(|g_i|, \eta) \right) \left(\sum_\eta a_\eta \frac{d^2 F}{d|g_i|^2} \right).$$

but since $F \times F'' \geq (F')^2$, pointwise, we have $\sqrt{F(|g_i|, \eta)} \sqrt{\frac{d^2 F}{d|g_i|^2}} \geq \frac{dF}{d|g_i|}$. Hence,

$$\left(\sum_\eta a_\eta \frac{dF}{d|g_i|} \right) \leq \left(\sum_\eta a_\eta \sqrt{F(|g_i|, \eta)} \sqrt{\frac{d^2 F}{d|g_i|^2}} \right).$$

The last two inequalities together yield:

$$\left(\sum_\eta a_\eta \frac{dF}{d|g_i|} \right)^2 \leq \left(\sum_\eta a_\eta F(|g_i|, \eta) \right) \left(\sum_\eta a_\eta \frac{d^2 F}{d|g_i|^2} \right),$$

which shows the numerator is non-negative. Therefore,

$$\frac{d^2 \alpha(\lambda)}{d|g_i|^2} \geq 0,$$

and $\alpha(\lambda)$ is Schur-convex. \square

We are now ready to prove Theorem 4.3.

Proof: We apply Schur's condition (also known as the Schur-Strowski criterion) to prove that $\alpha(\lambda)$ is Schur-convex. Recall that a symmetric function $f(x_1, \dots, x_n)$ is Schur-convex if and only if for all

$i \neq j$,

$$(x_i - x_j) \left(\frac{\partial f}{\partial x_i} - \frac{\partial f}{\partial x_j} \right) \geq 0.$$

In our case, the function is $\alpha(\lambda) = \sum_{i=1}^n \alpha_{\bar{g}_i}(\lambda)$, where \bar{g}_i is the noisy version of the ℓ_2 -clipped marginal gradients. Denote by \mathbf{g}_i , $i \in [n]$, marginal gradients after ℓ_2 clipping and before the addition of DP noise. Then, with Theorem 4.2, the univariate moments accountant for the i -th coordinate satisfies

$$\alpha_{\bar{g}_i}(\lambda) \leq \log \left[\sum_{\eta=0}^{\lambda+1} \binom{\lambda+1}{\eta} (1-\zeta)^{\lambda+1-\eta} \zeta^\eta F(|\mathbf{g}_i|, \eta) \right], \quad (26)$$

where the function $F(|\mathbf{g}_i|, \eta)$ is defined as

$$F(|\mathbf{g}_i|, \eta) = \frac{e^{\frac{(\eta-1)|\mathbf{g}_i|}{b}}}{2} + \frac{e^{-\frac{\eta|\mathbf{g}_i|}{b}}}{2} + \frac{e^{\frac{(\eta-1)|\mathbf{g}_i|}{b}} - e^{-\frac{\eta|\mathbf{g}_i|}{b}}}{2(2\eta-1)}. \quad (27)$$

Define the term inside the square brackets in Equation (26) as X . Then, the derivative of $\alpha_{\bar{g}_i}(\lambda)$ with respect to $|\mathbf{g}_i|$ satisfies

$$\frac{d\alpha_{\bar{g}_i}(\lambda)}{d|\mathbf{g}_i|} = \frac{\sum_{\eta=0}^{\lambda+1} \binom{\lambda+1}{\eta} (1-\zeta)^{\lambda+1-\eta} \zeta^\eta \frac{dF}{d|\mathbf{g}_i|}}{X}. \quad (28)$$

Lets compute the derivative $\frac{dF}{d|\mathbf{g}_i|}$:

$$\begin{aligned} \frac{dF}{d|\mathbf{g}_i|} &= \frac{(\eta-1)}{2b} e^{\frac{(\eta-1)|\mathbf{g}_i|}{b}} - \frac{\eta}{2b} e^{-\frac{\eta|\mathbf{g}_i|}{b}} \\ &+ \frac{1}{2(2\eta-1)} \left(\frac{(\eta-1)}{b} e^{\frac{(\eta-1)|\mathbf{g}_i|}{b}} + \frac{\eta}{b} e^{-\frac{\eta|\mathbf{g}_i|}{b}} \right). \end{aligned} \quad (29)$$

Special cases:

- For $\eta = 0$, the terms cancel symmetrically and $\frac{dF}{d|\mathbf{g}_i|} = 0$.
- For $\eta = 1$, the derivative simplifies to 0 by symmetry.
- For $\eta > 1$, expanding and grouping terms, we have

$$\frac{dF}{d|\mathbf{g}_i|} = \frac{(\eta-1)\eta}{b(2\eta-1)} \left(e^{\frac{(\eta-1)|\mathbf{g}_i|}{b}} - e^{-\frac{\eta|\mathbf{g}_i|}{b}} \right). \quad (30)$$

Since $\eta > 1$, the prefactor $\frac{(\eta-1)\eta}{b(2\eta-1)}$ is positive. Moreover, for any $|\mathbf{g}_i| \geq 0$, $e^{\frac{(\eta-1)|\mathbf{g}_i|}{b}} \geq e^{-\frac{\eta|\mathbf{g}_i|}{b}}$. Thus, $\frac{dF}{d|\mathbf{g}_i|} \geq 0$ for all \mathbf{g}_i and all η .

As stated earlier,

$$\frac{d\alpha_{\bar{g}_i}(\lambda)}{d|\mathbf{g}_i|} = \frac{\sum_{\eta=0}^{\lambda+1} \binom{\lambda+1}{\eta} (1-\zeta)^{\lambda+1-\eta} \zeta^\eta \frac{dF}{d|\mathbf{g}_i|}}{X}.$$

Since each $\frac{dF}{d|\mathbf{g}_i|} \geq 0$, $X > 0$, and all the coefficients are positive, it follows that

$$\frac{\partial \alpha(\lambda)}{\partial |\mathbf{g}_i|} \geq 0.$$

Since $\alpha(\lambda) = \sum_{i=1}^n \alpha_{\bar{g}_i}(\lambda)$ with each $\alpha_{\bar{g}_i}(\lambda)$ depending only on $|\mathbf{g}_i|$, we have $\frac{\partial \alpha(\lambda)}{\partial |\mathbf{g}_i|} = \frac{d\alpha_{\bar{g}_i}(\lambda)}{d|\mathbf{g}_i|}$. Thus, the overall moments accountant function (MAF) is non-decreasing. To satisfy the Schur–Ostrowski criterion, it suffices to show that the second derivative of $\alpha(\lambda)$ is non-negative (MAF is convex). A positive second derivative ensures that for any $i \neq j$, both $|\mathbf{g}_i| - |\mathbf{g}_j|$ and $\frac{\partial \alpha(\lambda)}{\partial |\mathbf{g}_i|} - \frac{\partial \alpha(\lambda)}{\partial |\mathbf{g}_j|}$ share the same sign, thereby satisfying the criterion. In Section B.1 we proved that the second derivatives are non-negative, concluding the proof for Theorem 4.3. \square

An *alternative* approach is to prove the Schur-convexity of the univariate MAF and apply the following results.

PROPOSITION B.2 (SCHUR[52]; HARDY–LITTLEWOOD–PÓLYA [28]). *Let $I \subset \mathbb{R}$ be an interval and $g : I \rightarrow \mathbb{R}$ be a convex function. Then the function*

$$\varphi(x) = \sum_{i=1}^n g(x_i)$$

is Schur-convex on I^n . Consequently, if $x \prec y$ on I^n , then

$$\varphi(x) \leq \varphi(y).$$

B.4 Proof of Lemma 4.4

In the following, we prove Lemma 4.4 on the majorization set for ℓ_2 clipped gradients.

Proof: Since the ℓ_2 clipping ensures that $\|\mathbf{g}\|_2 \leq C$, we have $|\mathbf{g}_i| \leq C = x_1$. Applying the AM–QM inequality to the first i marginal clipped gradients, we have

$$\frac{1}{i} \sum_{j=1}^i |\mathbf{g}_j| \leq \sqrt{\frac{1}{i} \sum_{j=1}^i (|\mathbf{g}_j|)^2} \leq \frac{C}{\sqrt{i}},$$

which implies

$$\sum_{j=1}^i |\mathbf{g}_j| \leq C\sqrt{i}.$$

On the other hand, the majorization set x satisfies

$$\sum_{j=1}^i x_j = C\sqrt{i},$$

since

$$\sum_{j=1}^i x_j = C(\sqrt{i} - \sqrt{0})$$

by telescoping the differences.

Thus, for each $i = 1, \dots, n$, we have

$$\sum_{j=1}^i |\mathbf{g}_j| \leq \sum_{j=1}^i x_j,$$

establishing that $|\mathbf{G}| \prec_w x$.

C PLRV Mechanism Proofs

C.1 Proof of Theorem 4.8

In the following, we prove a tight bound on the moments accountant function of univariate PLRV mechanisms, as stated in Theorem 4.8.

Proof: Let $J \in [n]$ denote the indices of elements randomly selected through mini-batch sub-sampling, where elements are included i.i.d. with sub-sampling probability $\zeta = L/N$. We express the distribution of $M_g(d', f)$ as a double-fold mixture.

Let $\mu_0(b)$ denote a PLRV distribution centered at \mathbf{g} , with scale distributed with $f(b)$. Thus $M_g(d, f) \sim \mu_0$.

Let $\mu_1(b)$ denote a PLRV distribution centered at the value of \bar{g} conditioned on the event $n \in J$. Then the distribution of $M_g(d', f)$ is the mixture $\mu_\Delta = (1 - \zeta)\mu_0(b) + \zeta\mu_1(b)$.

The MAF of the PLRV mechanism with a pre-specified (but arbitrary) pair $\{d, d'\}$ and using worst case sensitivity (to bound

over worst case aux), can be expressed as

$$\begin{aligned}\alpha_{M_g}(\lambda) &= \max\left(\alpha_{M_g}(\lambda; d, f), \alpha_{M_g}(\lambda; d', f)\right) \\ &= \log \max \left\{ \mathbb{E}_{z \sim \mu_0} \left[\left(\frac{\mu_0(z)}{\mu_\Delta(z)} \right)^\lambda \right], \mathbb{E}_{z \sim \mu_\Delta} \left[\left(\frac{\mu_\Delta(z)}{\mu_0(z)} \right)^\lambda \right] \right\},\end{aligned}\quad (31)$$

where we use that by monotonicity of logarithms,

$$\max\{\log a_1, \log a_2\} = \log \max\{a_1, a_2\}.$$

Similar to the argument in Proof B.2 (of Theorem 3.2), we multiply by $\mu_0(z)/\mu_0(z)$ and rearrange to obtain:

$$A = \mathbb{E}_{z \sim \mu_0(b)} \left[\left(\frac{\mu(z; b)}{\mu_0(z; b)} \right)^{\lambda+1} \right] = \mathbb{E}_{z \sim \mu_0(b)} \left[\left(1 - \zeta + \zeta \frac{\mu_1(z; b)}{\mu_0(z; b)} \right)^{\lambda+1} \right],$$

and

$$\begin{aligned}B &= \mathbb{E}_{z \sim \mu_0(b)} \left[\left(\frac{\mu_0(z; b)}{(1 - \zeta)\mu_0(z; b) + \zeta\mu_1(z; b)} \right)^\lambda \right] \\ &= \mathbb{E}_{z \sim \mu_0(b)} \left[\left(\frac{1}{1 - \zeta + \zeta \frac{\mu_1(z; b)}{\mu_0(z; b)}} \right)^\lambda \right].\end{aligned}$$

REMARK. The expressions for A and B are conditional (on b) variants of those in Proof B.2. By the law of total expectation, the bound on A becomes $\mathbb{E}_b[A(z | b)]$, which simplifies to:

$$A = \mathbb{E}_b \left[\exp\left(\frac{-\eta C}{b}\right) \cdot \frac{\eta - 1}{2\eta - 1} + \exp\left(\frac{(\eta - 1)C}{b}\right) \cdot \frac{\eta}{2\eta - 1} \right]. \quad (33)$$

This yields the bound:

$$A = \frac{\eta}{2\eta - 1} \mathcal{M}_u((\eta - 1)C) + \frac{\eta - 1}{2\eta - 1} \mathcal{M}_u(-\eta C),$$

where $u = 1/b$ is the reciprocal of the PLRV scale.

Thus, the moments accounting function satisfies:

$$\alpha_{M_g}(\lambda) = \log \left\{ \sum_{\eta=0}^{\lambda+1} \binom{\lambda+1}{\eta} (1 - \zeta)^{\lambda+1-\eta} \zeta^\eta \mathcal{G}(C, \eta) \right\}.$$

We proceed to formally prove the above result. Mironov et al. [42] (Section 3.1) demonstrate that $A \geq B$ holds in general for centrally symmetric distributions.

We begin by applying the binomial theorem,

$$\begin{aligned}B &= \mathbb{E}_{z \sim \mu_0} \left[\left(1 - \zeta + \zeta \frac{\mu_1(z)}{\mu_0(z)} \right)^{\lambda+1} \right] \\ &= \mathbb{E}_{z \sim \mu_0} \left[\sum_{\eta=0}^{\lambda+1} \binom{\lambda+1}{\eta} (1 - \zeta)^{\lambda+1-\eta} \left(\zeta \frac{\mu_1(z)}{\mu_0(z)} \right)^\eta \right] \\ &= \sum_{\eta=0}^{\lambda+1} \binom{\lambda+1}{\eta} (1 - \zeta)^{\lambda+1-\eta} \zeta^\eta \mathbb{E}_{z \sim \mu_0} \left[\left(\frac{\mu_1(z)}{\mu_0(z)} \right)^\eta \right]\end{aligned}$$

$$A = \mathbb{E}_{z \sim \mu_\Delta} \left[\left(1 - \zeta + \frac{\zeta \mu_1(z)}{\mu_0(z)} \right)^\lambda \right] = \mathbb{E}_{z \sim \mu_0} \left[\left(1 - \zeta + \frac{\zeta \mu_1(z)}{\mu_0(z)} \right)^{\lambda+1} \right],$$

$$B = \mathbb{E}_{z \sim \mu_0} \left[\left(\frac{\mu_0(z)}{(1 - \zeta)\mu_0(z) + \zeta\mu_1(z)} \right)^\lambda \right] = \mathbb{E}_{z \sim \mu_0} \left[\left(\frac{1}{1 - \zeta + \frac{\zeta \mu_1(z)}{\mu_0(z)}} \right)^\lambda \right]$$

Let us begin with "A." While A involves two cases— $\mu_0(z) \propto e^{-\frac{|z|_1}{b}}$ and $\mu_0(z) \propto e^{-\frac{|z-C|_1}{b}}$ —both yield the same bound, likely due to an underlying symmetry. Thus, we focus on the former.

Analysis for A:

$$A = \mathbb{E}_{z \sim \mu_0(b)} \left[\left(1 - \zeta + \zeta \cdot e^{-\frac{\|z-C\|_1 + \|z\|_1}{b}} \right)^{\lambda+1} \right],$$

To tackle each we must cover three cases, $z \geq c$, $z < 0$ and $z \in [0, C)$. We will first analyze easier $z \geq c$ and $z < 0$ cases and lastly derive the harder case $z \in [0, C)$.

Case A-I ($z \geq C$):

$$\begin{aligned}A &= \mathbb{E}_{\{[z \geq C] \sim \mu_0(b)\}} \left[\left(1 - \zeta + \zeta \cdot e^{C/b} \right)^{\lambda+1} \right], \\ A &= \mathbb{E}_{\{[z \geq C] \sim \mu_0(b)\}} \left\{ \sum_{\eta=0}^{\lambda+1} \binom{\lambda+1}{\eta} (1 - \zeta)^{\lambda+1-\eta} \zeta^\eta \cdot e^{\eta C/b} \right\} \\ A &= \sum_{\eta=0}^{\lambda+1} \binom{\lambda+1}{\eta} (1 - \zeta)^{\lambda+1-\eta} \zeta^\eta \cdot \mathbb{E}_{\{[z \geq C] \sim \mu_0(b)\}} \{e^{\eta C/b}\}\end{aligned}$$

Note that $e^{\eta C/b}$ has no variable z and purely written in terms of b . Thus we can plug the Laplace CDF followed by expectation over b . Precisely,

$$A = \sum_{\eta=0}^{\lambda+1} \binom{\lambda+1}{\eta} (1 - \zeta)^{\lambda+1-\eta} \zeta^\eta \cdot \mathbb{E}_{b \sim f(b)} \{ \mathbb{P}_{z \sim \text{Lap}(0, b)}(z \geq C) \cdot e^{\eta C/b} \}$$

but we know that $\mathbb{P}_{z \sim \text{Lap}(0, b)}(z \geq C) = 0.5e^{-C/b}$. Thus

$$A = \sum_{\eta=0}^{\lambda+1} \binom{\lambda+1}{\eta} (1 - \zeta)^{\lambda+1-\eta} \zeta^\eta \cdot \mathbb{E}_{b \sim f(b)} \{0.5e^{-C/b} \cdot e^{\eta C/b}\}$$

Given that the expectation is half of MGF at $(\eta - 1) \cdot C$, we have

$$A = 0.5 * \sum_{\eta=0}^{\lambda+1} \binom{\lambda+1}{\eta} (1 - \zeta)^{\lambda+1-\eta} \zeta^\eta \cdot \mathcal{M}_u((\eta - 1) \cdot C)$$

Case A-II ($z < 0$):

$$\begin{aligned}A &= \mathbb{E}_{\{[z < 0] \sim \mu_0(b)\}} \left[\left(1 - \zeta + \zeta \cdot e^{-\frac{C}{b}} \right)^{\lambda+1} \right], \\ A &= \mathbb{E}_{\{[z < 0] \sim \mu_0(b)\}} \left\{ \sum_{\eta=0}^{\lambda+1} \binom{\lambda+1}{\eta} (1 - \zeta)^{\lambda+1-\eta} \zeta^\eta \cdot e^{-\eta C/b} \right\} \\ A &= \sum_{\eta=0}^{\lambda+1} \binom{\lambda+1}{\eta} (1 - \zeta)^{\lambda+1-\eta} \zeta^\eta \cdot \mathbb{E}_{\{[z < 0] \sim \mu_0(b)\}} \{e^{-\eta C/b}\}\end{aligned}$$

Note that $e^{-\eta C/b}$ has no variable z and purely written in terms of b . Thus we can plug the Laplace CDF followed by expectation over b . Precisely,

$$A = \sum_{\eta=0}^{\lambda+1} \binom{\lambda+1}{\eta} (1-\zeta)^{\lambda+1-\eta} \zeta^\eta \cdot \mathbb{E}_{b \sim f(b)} \{ \mathbb{P}_{z \sim \text{Lap}(0,b)}(z < 0) \cdot e^{-\eta C/b} \}$$

but we know that $\mathbb{P}_{z \sim \text{Lap}(0,b)}(z < 0) = 0.5$. Thus

$$A = \sum_{\eta=0}^{\lambda+1} \binom{\lambda+1}{\eta} (1-\zeta)^{\lambda+1-\eta} \zeta^\eta \cdot \mathbb{E}_{b \sim f(b)} \{ 0.5 \cdot e^{-\eta C/b} \}$$

Given that the expectation is half of MGF at $-\eta \cdot C$, we have

$$A = 0.5 * \sum_{\eta=0}^{\lambda+1} \binom{\lambda+1}{\eta} (1-\zeta)^{\lambda+1-\eta} \zeta^\eta \cdot \mathcal{M}_u(-\eta \cdot C)$$

Case A-III ($0 \leq z < C$):

$$A = \mathbb{E}_{\{0 \leq z < C\} \sim \mu_0(b)} \left[\left(1 - \zeta + \zeta \cdot e^{\frac{2z-C}{b}} \right)^{\lambda+1} \right],$$

$$A = \sum_{\eta=0}^{\lambda+1} \binom{\lambda+1}{\eta} (1-\zeta)^{\lambda+1-\eta} \zeta^\eta \cdot \mathbb{E}_{\{0 \leq z < C\} \sim \mu_0(b)} \{ e^{\frac{\eta(2z-C)}{b}} \}$$

So we need to calculate $\mathbb{E}_{\{0 \leq z < C\} \sim \mu_0(b)} \{ e^{\frac{\eta(2z-C)}{b}} \}$ which can be written as a sequence of two expectations (law of total expectation):

$$\mathbb{E}_{b \sim f(b)} \mathbb{E}_{z \sim \text{Lap}(0,b)} \{ e^{\frac{\eta(2z-C)}{b}} \} = \mathbb{E}_{b \sim f(b)} \left\{ \int_0^C \frac{e^{\frac{\eta(2z-C)-|z|}{b}}}{2b} dz \right\}$$

We focus on the one-dimensional Laplace distribution in our analysis to simplify the presentation and avoid excessive jargon. The extension to the multi-dimensional case follows straightforwardly. Calculating the integral is easy and it is given as:

$$\int_0^C \frac{e^{\frac{z(2\eta-1)-(C\eta)}{b}}}{2b} dz = \frac{e^{\frac{C(2\eta-1)-(C\eta)}{b}} - e^{\frac{-C\eta}{b}}}{2 * (2\eta - 1)}$$

Moving forward with the expectation:

$$\mathbb{E}_{b \sim f(b)} \left\{ \frac{e^{\frac{C(\eta-1)}{b}} - e^{\frac{-C\eta}{b}}}{2 * (2\eta - 1)} \right\} = \frac{\mathcal{M}_u(C(\eta - 1)) - \mathcal{M}_u(-C\eta)}{2 * (2\eta - 1)}$$

Combining the results in Cases A-I, A-II and A-III, we have that $A = \frac{\eta}{2\eta-1} \mathcal{M}_u((\eta-1)C) + \frac{\eta-1}{2\eta-1} \mathcal{M}_u(-\eta C)$ concluding the proof.

Analysis for B: Following the argument in Proof B.2 (Theorem 3.2), and using binomial expansion with term-wise comparison, we find that $B \geq A$, consistent with the result of Mironov et al.

C.2 Justifying Differentiation (Leibniz's Rule)

In the proof of Theorem 5.1 (presented in Section C.3), we will use Leibniz's rule for differentiation under the integral sign. For completeness, we now discuss the conditions under which this holds.

We use Leibniz's rule for differentiation under the integral sign:

$$\frac{d}{du} \int_{\mathbb{R}^k} f(u, O) dO = \int_{\mathbb{R}^k} \frac{\partial f(u, O)}{\partial u} dO,$$

which is valid under the following conditions: 1. Continuity of the Integrand: The function $f(u, O) = e^{-u \cdot \|O - \tilde{g}_t(d)\|_1}$ is continuous with respect to $u > 0$ and $O \in \mathbb{R}^k$. 2. Existence and Continuity of the Derivative: The partial derivative $\frac{\partial f(u, O)}{\partial u} = -\|O - \tilde{g}_t(d)\|_1$

$\tilde{g}_t(d)\|_1 e^{-u \cdot \|O - \tilde{g}_t(d)\|_1}$ exists and is continuous. 3. Convergence of the Integral: The integral

$$\int_{\mathbb{R}^k} e^{-u \cdot \|O - \tilde{g}_t(d)\|_1} dO$$

converges for all $u > 0$, as the exponential decays rapidly for large $\|O - \tilde{g}_t(d)\|_1$. 4. No Divergence from the Derivative: The derivative $-\|O - \tilde{g}_t(d)\|_1 e^{-u \cdot \|O - \tilde{g}_t(d)\|_1}$ does not cause divergence because the exponential decay ensures the integral remains finite.

Since these conditions are met, applying Leibniz's rule to move $\frac{d}{du}$ outside the inner integral is valid.

C.3 Proof of Theorem 5.1

Proof: The ℓ_1 error is defined as:

$$\ell_1(z) = \mathbb{E}[\|z - \tilde{g}_t(d)\|_1].$$

Using the PDF $g(u)$ of the inverse scale parameter u , it can be rewritten as:

$$\ell_1(z) = \int_0^\infty g(u) \int_{\mathbb{R}^n} \|z - \tilde{g}_t(d)\|_1 e^{-u \|z - \tilde{g}_t(d)\|_1} dz du.$$

a) applying Leibniz's rule, which permits differentiation under the integral sign (see Appendix C.2 for condition verification), and using the identity $\|z - \tilde{g}_t(d)\|_1 e^{-u \|z - \tilde{g}_t(d)\|_1} = -\frac{d}{du} e^{-u \|z - \tilde{g}_t(d)\|_1}$,

b) moving $\frac{d}{du}$ outside the inner integral:

$$\ell_1(z) = \int g(u) \left(\frac{u}{2} \right)^n \left(-\frac{d}{du} \int_{\mathbb{R}^n} e^{-u \|O - \tilde{g}_t(d)\|_1} dO \right) du,$$

and c) integrating by parts yields: $\ell_1(z) = \int_0^\infty \frac{g(u)}{u} du$.

D Further Discussion

D.1 Interpreting PLRV-O Parameters

Theta - Learnability. Table 11 highlights the role of the θ parameter in model learnability under privacy constraints. By varying the θ while keeping all other hyperparameters fixed, we have observed a clear understanding of θ dependency on model performance. Smaller values of θ led to significantly lower performance, while larger values of θ substantially improved the model performance. Therefore, θ can be observed as a sensitivity control parameter, with larger values offering good model learnability in our setting.

K - Utility Parameter. Table 12 shows that the accuracy of PLRV-O boosts with higher values of k . This suggests that k serves as a utility parameter, improving the model performance under DP.

Table 11: CNN-MNIST: Memorization threshold dependency on θ . Fixed parameters: $\delta = 10^{-5}$, $\text{Clip} = 3$, $q = 0.01$, $\text{Steps} = 300$. Larger θ values are less destructive in this setting. Small theta values can lead to either unstable models or highly protected yet accurate ones. PLRV-O Acc averaged over 5 trials.

ϵ	k	θ	PLRV-O Acc
0.0457	1418	1.01E-05	18.456±1.87
0.7971	1418	1.01E-04	64.174±4.43
238.10	1418	1.01E-03	93.658±0.34

Table 12: CNN-MNIST: Model quality enhances with k . PLRV-O Acc taken over 5 trials and averaged. Fixed parameters: $\delta = 10^{-5}$, $\theta = 1.01E - 03$, **Clip = 1, $q = 0.01$, **Steps = 300**.**

ϵ	k	PLRV-O Acc
1.0691	500	87.614±1.34
4.1055	1000	92.146±0.91
8.3310	1390	93.792±0.57
8.7180	1418.922	93.634±0.79
8.8879	1430	93.702±0.63
9.9292	1500	93.438±0.42
20.4878	2000	94.13±0.49
66.5293	3000	95.114±0.22
363.376	5000	96.00±0.45
2.23E+03	10000	96.212±0.40

D.2 Tighter Search Space for PLRV-O

PLRV-O finetuning for larger models, e.g., >100M parameters, is a harder problem to solve. We propose an approach to constructing the PLRV-O search space by filtering candidate configurations against a Gaussian DP-SGD baseline. A configuration is retained only if it achieves both (i) lower moment values at every order and (ii) lower distortion than its Gaussian counterpart.

THEOREM D.1 (THE PLRV-O SEARCH SPACE). *Given a training dataset \mathcal{D} , task configuration $\mathbf{x} = (E, B, C)$, and privacy parameters (ϵ, δ) , the PLRV-O search space $SS(\mathbf{x}, \epsilon, \delta)$ is defined as:*

$$SS(\mathbf{x}, \epsilon, \delta) = \left\{ \Theta(\mathbf{x}) \mid \mathbb{I}_{DP}(\Theta(\mathbf{x}), \eta, \epsilon, \delta) \wedge \mathbb{I}_{Dist}(\Theta(\mathbf{x}), \epsilon, \delta) = 1 \right\}$$

where the indicators enforce per-moment privacy bounds and distortion constraints:

$$\mathbb{I}_{DP}(\Theta, \eta, \epsilon, \delta) = \begin{cases} 1, & \forall \eta \in \mathbb{N} : \mathcal{G}(u(\Theta(\mathbf{x})), \eta) \leq \exp\left(\frac{\eta^2 - \eta}{2\sigma^2(\mathbf{x}, \epsilon, \delta)}\right) \\ 0, & \text{otherwise} \end{cases}$$

$$\mathbb{I}_{Dist}(\Theta, \mathbf{x}, \epsilon, \delta) = \begin{cases} 1, & \int_0^\infty \mathcal{M}_{u(\Theta)}(-z) dz \leq \sqrt{\frac{2}{\pi}} C \sigma(\mathbf{x}, \epsilon, \delta) \\ 0, & \text{otherwise} \end{cases}.$$

In the case of $\Gamma(k, \theta)$ -PLRV noise, the feasible region can be characterized analytically. The following corollary provides closed-form bounds for k , conditioned on C , θ , and the maximum moment order λ_{max} .

COROLLARY D.2 (THE Γ -PLRV SEARCH SPACE). *Given task configuration $\mathbf{x} = (E, B, C)$ and privacy parameters (ϵ, δ) , the valid $\Gamma(k, \theta)$ -PLRV configurations satisfy:*

$$k_1(C, \theta, \eta) \leq k \leq k_2(C, \theta, \eta), \quad \forall \eta \leq \lambda_{max} + 1,$$

subject to $\theta < \frac{1}{C(\lambda_{max}+1)}$ and $k > 1$, where:

$$k_{1,2}(C, \theta, \eta) = \frac{4 \log(1 - C\theta(\eta - 1)) \mp \sqrt{\Delta}}{2C^2\theta^2(\eta - \eta^2)},$$

and $\Delta = 16 \log^2(C\theta - C\eta\theta + 1) + 11.09375 \cdot C^2\theta^2(\eta - \eta^2)$.

Proof: We have $\theta < \frac{1}{C(\lambda+1)}$ to ensure existence of MGF for the Γ -PDF. For the Γ -PLRV mechanism, the indicator functions specialize

to

$$\mathbb{I}_{DP}(k, \theta, \eta, \epsilon, \delta) = \begin{cases} 1, & \forall \eta \in \mathbb{N} : \mathcal{G}(C, k, \theta, \eta) \leq \exp\left(\frac{\eta^2 - \eta}{2\sigma^2(\mathbf{x}, \epsilon, \delta)}\right) \\ 0, & \text{otherwise} \end{cases}$$

$$\mathbb{I}_{Dist}(k, \theta, \mathbf{x}, \epsilon, \delta) = \begin{cases} 1, & \frac{1}{(k-1)\theta} \leq \sqrt{\frac{2}{\pi}} C \sigma(\mathbf{x}, \epsilon, \delta) \\ 0, & \text{otherwise} \end{cases}$$

where

$$\mathcal{G}(C, k, \theta, \eta) = \frac{(1 - (\eta - 1)C\theta)^{-k} + (1 + \eta C\theta)^{-k}}{2} + \frac{(1 - (\eta - 1)C\theta)^{-k} - (1 + \eta C\theta)^{-k}}{2(2\eta - 1)}.$$

Using the bound for \mathbb{I}_{Dist} , we have

$$\frac{1}{(k-1)\theta} \leq \sqrt{\frac{2}{\pi}} C \sigma(\mathbf{x}, \epsilon, \delta)$$

$$\implies \frac{1}{\sigma} \leq \sqrt{\frac{2}{\pi}} C(k-1)\theta. \quad (34)$$

Applying Equation (34) in $\mathbb{I}_{DP}(k, \theta, \eta, \epsilon, \delta)$ we have that for every $\eta \in \mathbb{N}$,

$$\mathcal{G}(C, k, \theta, \eta) \leq \exp\left(\frac{\eta^2 - \eta}{\pi} C^2(k-1)^2\theta^2\right).$$

Strictly speaking, due to the inequality direction in Equation (34), this yields a larger region than that characterized for a particular σ . However, this nonetheless yields a well-defined search space purely in terms of Γ -PLRV parameters k and θ .

Intersecting with c_0 - c_4 . To ensure practical feasibility, we further intersect this region with the heuristic constraints described earlier:

- c_0 Clip bounded: $C_{min} \leq C \leq C_{max}$.
- c_1 Gamma tail: $\theta \geq \theta_{min}(k) \leftarrow \text{GammaCDF}(0.1; k, \theta) < 1$.
- c_2 (Deferred here) privacy accounting via $\tau(\epsilon)$.
- c_3 Stability: $k > 1$.
- c_4 Distortion cap: $(k-1)\theta > 0.1$.

Together, the feasible region is characterized by

$$\max\{\theta_{min}(k), \frac{0.1}{k-1}\} \leq \theta < \frac{1}{\lambda_{max}C}, \quad k > 1, \quad C_{min} \leq C \leq C_{max},$$

with the objective of maximizing $(k-1)\theta$ (equivalently minimizing distortion). In practice, accounting further constrains the product $(k-1)\theta$ by requiring

$$(k-1)\theta \leq \tau(\epsilon).$$

As illustrated in Figure 14, $\tau(\epsilon)$ grows approximately in proportion to $k\theta$, highlighting the condition under which feasible configurations concentrate.

This result reduces the search region, allowing solvers to focus on feasible, high-quality configurations.

Figure 13 visualizes this search space for T, ζ, n required for NLP task MNLI, showing how optimal configurations evolve with varying task size and budget.

Nonlinear Solver over the Feasible Search Space. Given the pruned search space defined by constraints c_0 - c_4 , we optimize the SNR objective $J(k, \theta, C) = C(k-1)\theta$ using `fmincon`, MATLAB's solver for constrained nonlinear minimization [47]. The feasible set is specified via bound constraints on (k, θ, C) , together with

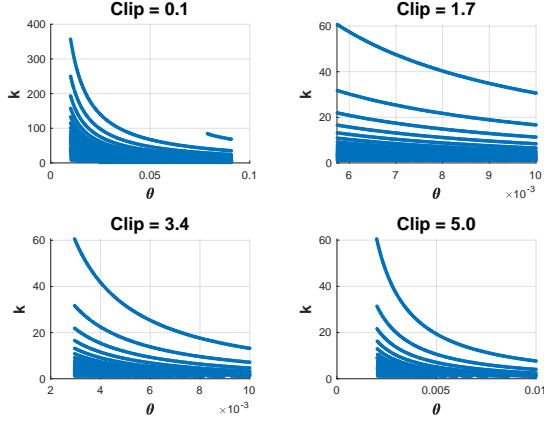


Figure 13: Γ -PLRV-O SS

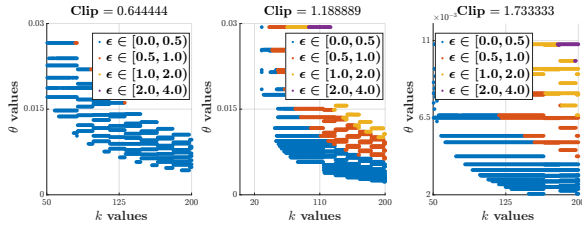


Figure 14: Search space for configurations in an MNLI task.

nonlinear constraints encoding the Gamma CDF cutoff, distortion threshold, and MGF validity. `fmincon` flexibly handles such problems and provides multiple backends, including the interior-point method [11], sequential quadratic programming (SQP) [5], and trust-region reflective methods [10]. This allows us to directly search within $SS(\mathbf{x}, \epsilon, \delta)$ and obtain (k^*, θ^*, C^*) .

Gradient Boosting for Parameter Prediction. To generalize PLRV-O configuration beyond explicitly optimized settings, one idea to explore is a regression-based prediction layer. For instance, training a Gradient Boosting Regression model, an ensemble method that incrementally improves predictions by fitting decision tree learners to residual errors. At iteration m , the predictor is updated as $F_m(x) = F_{m-1}(x) + \eta h_m(x)$, where $h_m(x)$ is the weak learner and η is the learning rate. The model takes $(k, \epsilon, C, T, \zeta)$ as inputs and predicts the corresponding noise parameter θ . This predictive layer captures nonlinear dependencies between training/privacy parameters and the optimal θ , and provides feature-importance scores that highlight which inputs most strongly influence the choice of noise parameters.

Together, the nonlinear solver and boosting predictor form a hybrid system: `fmincon` yields high-fidelity solutions within a constrained region, while gradient boosting extends coverage to unseen settings by learning patterns in previously optimized configurations.

PLRV-O and Neural Collapse. Recent work [60] highlights that DP-SGD training can induce *neural collapse*—a phenomenon where class representations become degenerate—particularly under strong privacy budgets. This occurs when DP noise overwhelms inter-class variation, flattening feature geometry. Since PLRV-O supports adaptive noise shaping via parameters k , θ , and C , it enables more

Algorithm 3 PLRV-O DP-SGD φ_2

Input: Data set d with size $|d|$, Initial model parameters Φ_0 , Loss $\mathcal{L}(\Phi)$, Learning rate lr , Clipping threshold C , Number of epochs E , Batch size B , PLRV-O Parameterization φ_1 , Privacy budget (ϵ^*, δ^*) , Population N , PLRV-O noise generator \mathcal{P}

Output: Model parameters Φ_T

// Initialization

- 1: Load model parameters Φ_0
- 2: Sampling rate $\zeta \leftarrow B/|d|$
- 3: Number of iterations $T \leftarrow \lceil E/q \rceil$
- 4: $(k^*, \theta^*, \hat{\epsilon}) \leftarrow \varphi_1(\epsilon^*, \tau, T, \zeta, C, N, \delta^*)$

// Main loop

- 5: **for** $t = 1$ **to** T **do**
 - 6: Draw a batch \mathcal{B}_t uniformly at random, where each element is included independently with probability ζ .
 - 7: **for** $\mathbf{x}_i \in \mathcal{B}_t$ **do**
 - 8: $\mathbf{g}_t(\mathbf{x}_i) \leftarrow \nabla_{\Phi} \mathcal{L}(\mathbf{x}_i)$
 - 9: $\tilde{\mathbf{g}}_t(\mathbf{x}_i) \leftarrow \mathbf{g}_t(\mathbf{x}_i) \cdot \min\left(1, \frac{C}{\|\mathbf{g}_t(\mathbf{x}_i)\|_2}\right)$
 - 10: $z \sim \mathcal{P}(k^*, \theta^*)$ // draw PLRV-O noise
 - 11: $\tilde{\mathbf{g}}_t \leftarrow \frac{1}{B} \sum_{\mathbf{x}_i \in \mathcal{B}_t} \tilde{\mathbf{g}}_t(\mathbf{x}_i) + z$
 - 12: $\tilde{\mathbf{g}}_t + 1 \leftarrow \text{Optimizer}(\tilde{\mathbf{g}}_t)$ // Where Optimizer is a DP-ready optimizer, such as AdamUpdate from [39]
 - 13: **return** Φ_T
-

controlled distortion and finer-grained modulation of the injected noise. By minimizing expected ℓ_1 distortion, PLRV-O better preserves representational diversity during training, reducing the risk of collapse in the latent space and sustaining learning signal even in high-dimensional settings.

D.3 Auditing DP-SGD

We consider two adversary models: a worst-case *theoretical DP adversary* and a practical *empirical auditing adversary*.

The Theoretical DP adversary has unbounded computation, full access to mechanism outputs, and arbitrary auxiliary knowledge. Privacy is formalized by (ϵ, δ) -DP, which bounds the effect of any single record on the output distribution.

Real deployments face constrained attackers. We used DP auditing tools that execute practical tests (e.g., canary-based inference) under limited queries or partial distributional knowledge, estimating empirical privacy via hypothesis testing (e.g., Type-II error-based criteria) while tracking the utility–noise trade-off.

ClipBKD. For ClipBKD, we run $T=500$ trials on CV tasks and $T=10$ on NLP tasks with confidence level 0.01 (99% confidence), and report the best result using $k=1$ poisoning point. For context, we also report (i) the best theoretical upper bound on ϵ and (ii) $\epsilon_{\text{OPT}}(500, 0.01)$, the best achievable lower bound ϵ_{LB} under T trials at confidence 0.01.

E Additional Information

E.1 Experimental Setting

Our experiments were conducted on the following servers:

- AMD Ryzen Threadripper PRO 5975WX 32-Core CPU, 500 GB RAM, and 3×NVIDIA Quadro RTX A6000 48GB GPUs.
- AMD EPYC 9354 32-Core Processor (128 cores), 1.5 TB RAM, and 2×NVIDIA H100 PCIe 80GB GPUs.

E.2 Additional Results

Tables 13-14 present additional evaluations of the performance of the PLRV-O framework on CNN-MNIST.

Table 13: PLRV-O performance on CNN-MNIST in high privacy regimes $\epsilon \leq 1.6$. Fixed parameters: $\delta = 10^{-5}$, $q = 0.01$, steps = 300. Gaussian baseline included and non-private (NP) accuracy range 96-98%. PLRV-O accuracy was taken over 5 trials and averaged.

ϵ	Clip	θ	k	Gauss Acc	PLRV-O Acc
0.065	0.1	1.00E-05	60000	66.56±6.37	88.78±1.06
0.171	0.1	5.00E-05	30000	82.20±2.40	93.38±0.90
0.284	0.3	8.00E-05	10000	88.53±2.11	89.96±0.95
0.596	0.3	8.00E-04	20000	91.44±1.65	93.85±0.74
0.757	0.3	5.00E-04	40000	92.26±0.26	94.30±0.51
0.921	0.3	6.00E-04	40000	92.65±0.46	94.81±0.13
0.962	0.5	3.00E-04	50000	92.87±0.35	93.69±0.56
1.172	0.5	3.00E-05	60000	92.78±0.18	94.37±0.65
1.606	0.5	6.00E-05	40000	93.73±0.43	94.91±0.43

Table 14: PLRV-O performance on CNN-Fashion-MNIST in high privacy regimes $\epsilon \leq 1.6$. Fixed parameters: $\delta = 10^{-5}$, $q = 0.01$, steps = 300. Gaussian baseline included and non-private (NP) accuracy range 82-83%. PLRV-O accuracy was taken over 5 trials and averaged.

ϵ	Clip	θ	k	Gauss Acc	PLRV-O Acc
0.065	0.1	1.00E-05	60000	59.28±2.79	70.72±0.61
0.171	0.1	5.00E-05	30000	68.19±1.91	73.42±1.49
0.284	0.3	8.00E-05	10000	69.77±1.67	72.34±0.82
0.596	0.3	8.00E-04	20000	72.34±0.67	73.67±1.29
0.757	0.3	5.00E-04	40000	72.64±0.79	74.57±0.56
0.921	0.3	6.00E-04	40000	73.57±0.64	75.49±0.82
0.962	0.5	3.00E-04	50000	73.24±0.61	74.48±0.57
1.172	0.5	3.00E-05	60000	73.04±0.84	74.72±0.90
1.606	0.5	6.00E-05	40000	74.25±0.53	76.25±0.73